ASSOCIATION POUR LE DÉVELOPPEMENT DE L'ENSEIGNEMENT
ET DE LA RECHERCHE EN SYSTÉMATIQUE APPLIQUÉE

MELISSA

Study for the non linear Model Based Predictive Control of Spirulina compartment using knowledge model

***

Contract ESA-ESTEC / ADERSA
Purchase order n° 142356 of 30/06/94

****

Technical Note 24.1

N. FULGET

- February 1995 -

7, Bd du Maréchal Juin
B.P. 52
91371 VERRIERES-LE-BUISSON CEDEX
Tél. (1) 60.13.53.53
Télécopieur (1) 69.20.05.63

ADERSA

SUMMARY

I - INTRODUCTION

The first contract between ESA-ESTEC and ADERSA, concerning MELISSA, was held in 1993 (contract n° PRF 132443 - First approach of Model Based Predictive Control of Spirulina compartment).

The results have been presented in TN 21.1 and TN 21.2.

They concern the elaboration of a Simulink simulator of the Spirulina compartment, and the design and tests of a linear predictive control on the simulator (TN 21.1).

At the end of the study, the knowledge model, developped in LGCB, at Clermont-Ferrand (TN 19.1, TN 19.2, TN 19.3) was integrated in the Simulink simulator (TN 21.2).

The first part of this study has consisted in the knowledge model validation. The experimental results have been compared to simulation results for different dilution rates.

In the second part of the study, we have developped a non linear Model Based Predictive Control law, and a hierarchical control strategy. Those have been tested on the knowledge model simulator.

II - MODEL VALIDATION

In TN 21.2, the Simulink simulator using the knowledge model has been validated, in comparison to the simulator developped in LGCB, named PHOTOSIM.

This validation has been done to insure that there were no programming problems.

At the beginning of this study, the purpose was to validate the model, compared to the experimental results.

Experimental results have been obtained on the photosynthetic reactor in ESTEC. The protocols applied on this reactor were steps of light energy, at different dilution rates.

At the beginning of the study, the concentration was supposed to be controlled by the action of the pump. But, considering the whole loop MELISSA, it is better to suppose that the flow is given by the upper level (hierarchical strategy). Then the concentration can not be maintained at a fixed value.

The production is the product of the concentration with the flow. If we suppose that the flow is fixed, the dynamic of production is the same as the dynamic of concentration.

When a step of light is applied on the reactor, the concentration is stabilized at a new value, after several hundred hours. This dynamics depends on the concentration value and on the dilution rate.

The protocols are done during one or two weeks, in order to have the complete dynamic response.

To validate the model, it is necessary to apply different protocols on the process. Those protocols are different steps of light, for different dilution rates. They have to be applied during one or two weeks because of the dynamics.

- For a step of light from 110 W/m^2 to 210 W/m^2, with a dilution rate equal to 0.018 h^{-1}, the results obtained on the simulator are similar to experimental results *(figure 1)*. The time response (at 95 %) is about 150 hours.

- For the same step of light, but with a dilution rate equal to 0.0103 h^{-1}, the behaviour of the simulator has the same gain as in experimental situation, but the experimental results are more dynamic *(figure 2)*. In experimental case, the time response is about 150 hours (with an overshoot). In simulation, the time response is about 300 hours, but the gain is the same as in experimental case.

- For a high dilution rate (0.03 h^{-1}), the results obtained on the simulator are different from the experimental results.

  Other tests at high dilution rate have to be done.

  But the model seems to be sufficiently reliable to be used in the control algorithm.

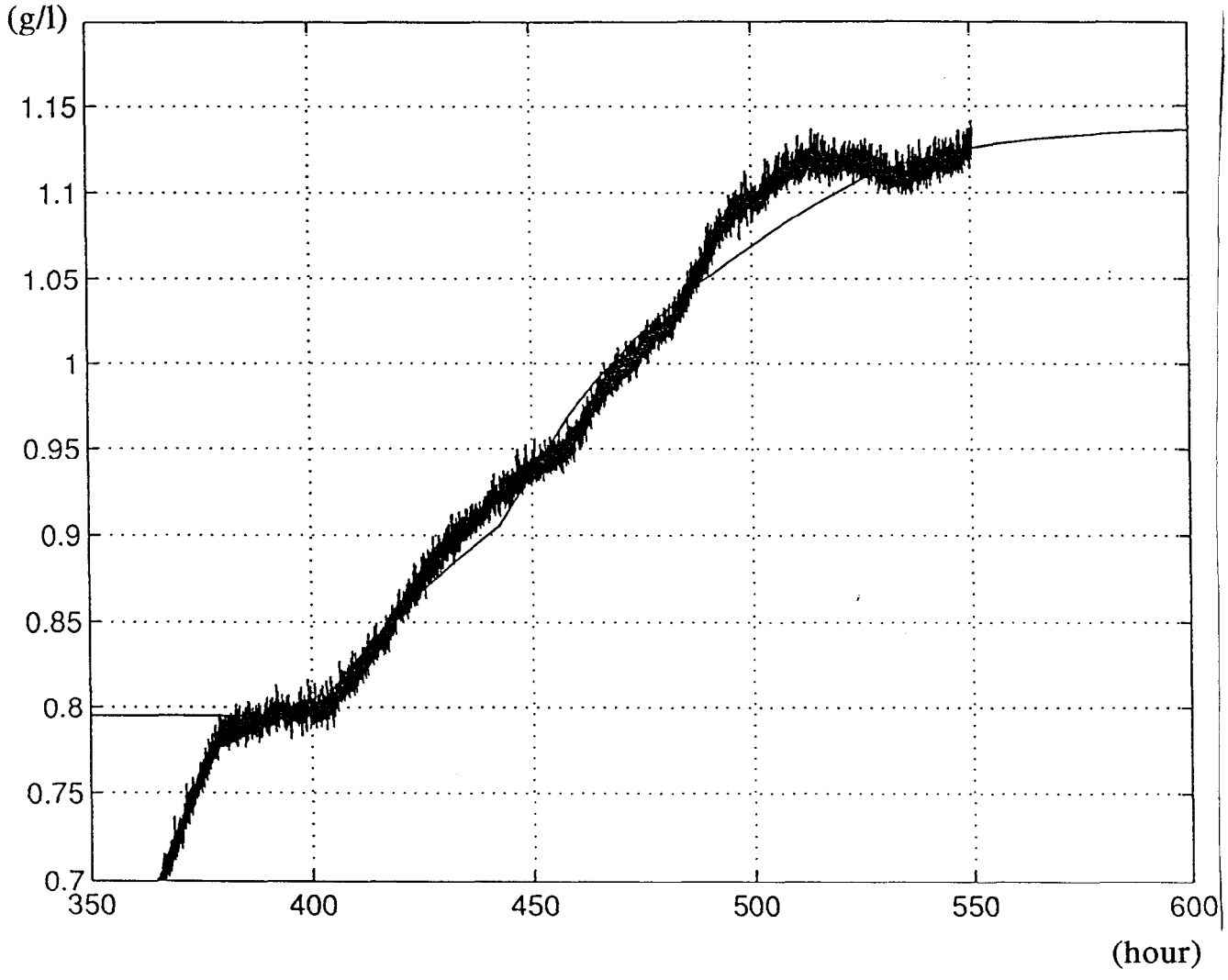

Figure 1 :

Active biomass concentration - Step of F_r
(Dil = 0.018 h^{-1} - F_r = 110 to 210 W/m^2)

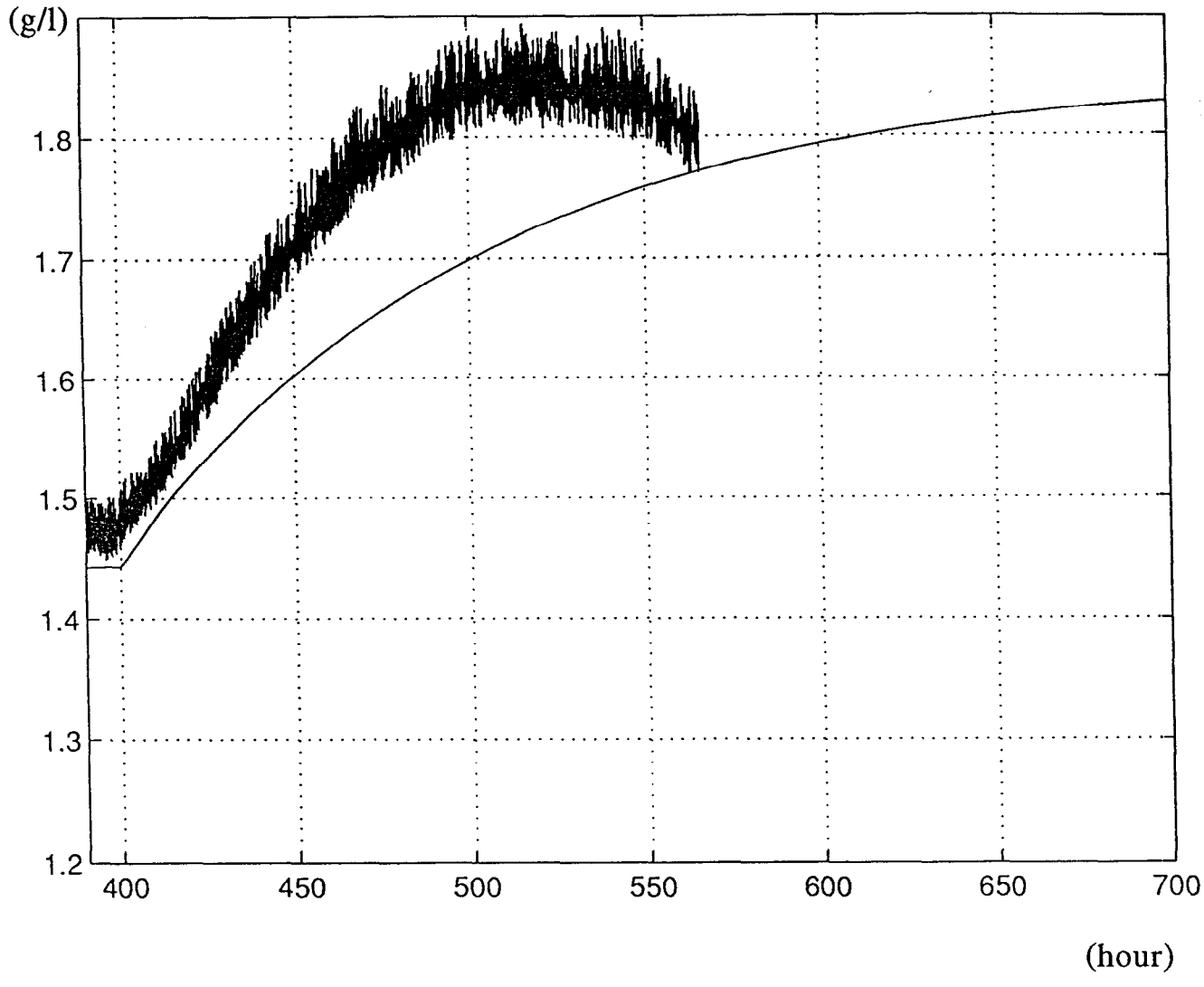

Figure 2 :

Active biomass concentration - Step of F_r
(Dil = 0.0103 h^{-1} - F_r = 112 to 210 W/m^2)

III - HIERARCHICAL STRATEGY

III.1 - General presentation

In this study, we are concerned with the control of the biomass production in the MELISSA Spirulina compartment (IV). But, we can't do it efficiently without considering the whole loop MELISSA, and especially the previous compartment (III), which will feed the Spirulina compartment. That is why we consider a hierarchical control strategy, which will be integrated more easily in the global control strategy.

The hierarchical strategy that has been developped is described hereafter. It is separated in 3 levels. We present the level 1 in more details.

III.2 - Level 0

This level concerns the control of the light intensity. It could be in open loop : a setpoint of radiant flux is applied, and it is supposed to be realized.

If we want to control in closed loop, it supposes that a value of radiant flux F_r is available. But in fact the only measurement of light intensity is E_b (the light intensity in the center of the reactor). So, a relation between E_b and F_r has to be used. This relation has been developped by BINOIS (CNAM thesis 1994). It is also a function of the biomass concentration C_{XA}. The level 0 can be described by the figure 3.

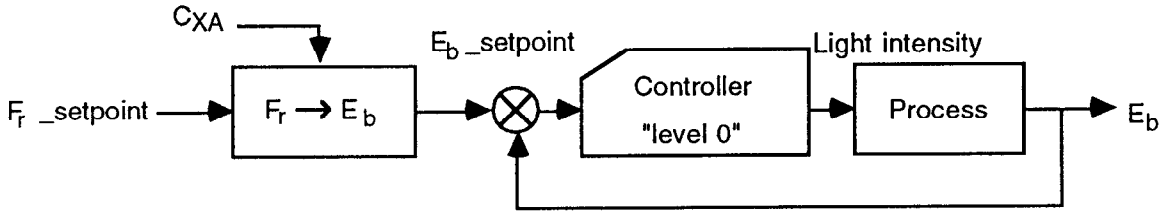

Figure 3

As the relation between E_b and F_r seems to be available, this solution is certainly more efficient than the open loop solution.

It will be interesting to test both solutions on the process and to compare each other objectively.

In the simulation tests, the level 0 has been supposed to be perfect : the radiant flux setpoint (calculated by the level 1) is directly applied on the process. The real radiant flux is supposed to be equal to the radiant flux setpoint.

III.3 - Level 1

This level is based on a predictive control strategy. The control structure is the following one :

The **Manipulated Variable** (MV), which is the control action, is the radiant flux setpoint F_r. It is the output of the level 1, and the input of the level 0. The radiant flux is expressed in W/m^2.

The **Controlled Variable** (CV) is the biomass production (in g/h). It is defined by the product of the biomass concentration with the flow :

$$\underset{(g/h)}{prod} = \underset{(g/l)}{C_{XA}} \cdot \underset{(l/h)}{q_e} \qquad \text{(III.1)}$$

with : C_{XA} : biomass concentration
q_e : input flow

The **Disturbance Variable** (DV) is the flow q_e (in l/h). Indeed, it is a second input of the system, which is measured, and can be taken into account in the prediction.

<u>The method</u>

The method is based on the PFC method principles, but applied with a non linear model.

The basic principles of PFC method are presented in Annex A. They are listed hereafter :

- internal model ;
- reference trajectory ;
- manipulated variable structuration ;
- modelling error extrapolation.

When the model is linear, the superposition principle can be used to calculate the prediction of the model output. But when the chosen model is non linear, it is no more possible to use the superposition principle. Then, one of the methods that can be used is named the scenario strategy. It consists in the application of several input protocols on the non linear model, to calculate the prediction of the model output.

In this application, the input protocol (radiant flux) and the flow protocol are supposed to be constant on the whole prediction horizon.

The reference trajectory defines the rallying to the setpoint. It is a first order reference trajectory. Its time response TR is a tuning parameter. The value of the reference trajectory at the coïncidence point h_c defines the control objective :

$$prod\_ref(n+h_c) = cons\_prod(n+h_c) - \lambda^{h_c} . (cons\_prod(n) - prod(n)) \quad (III.2)$$

with : $\lambda = \exp\left(\frac{-3dt}{TR}\right)$

dt : control period

prod(n) is the measured production at current time

The production setpoint $cons\_prod(n+h_c)$ on the coïncidence point h_c is supposed to be equal to the current production setpoint cons_prod(n).

So :

$$prod\_ref(n+h_c) = cons\_prod(n) - \lambda^{h_c} . (cons\_prod(n) - prod(n)) \quad (III.3)$$

$prod\_ref(n+h_c)$ is the control objective. So, we have to calculate the value of radiant flux which would give a production equal to $prod\_ref(n+h_c)$ at time $n+h_c$.

To determine it, the results of the scenarios applied on the model are used.

For each scenario, the model is running from n to $n+h_c$, with the flow equal to the measured value at current time n, and with a certain value of radiant flux F_r.

- A first scenario is applied with F_{r1} equal to the radiant flux applied to the process at previous control time.
- A second scenario is applied to the model with another value of radiant flux.

$$F_{r2} = F_{r1} + dF_r . sign(cons\_prod(n) - prod(n)) \quad (III.4)$$

In this version, the value of the difference dF_r between the two radiant flux scenarios F_{r1} and F_{r2} is arbitrary fixed, but the sign depends on the sign of the difference between real production and production setpoint.

In a future version, it would be possible to determine the value of dF_r with statical considerations.

Applying F_{r1} on the model gives a value of production equal to $prod_1(n+h_c)$ at time $n+h_c$. Applying F_{r2} gives a production equal to $prod_2(n+h_c)$ at time $n+h_c$.

We consider that the relation between F_r and $prod(n+h_c)$ is locally linear and then, the value of radiant flux that would have given a production equal to $prod\_ref(n+h_c)$ is calculated by the formula :

$$F_r = F_{r1} + \frac{(prod\_ref(n+h_c) - prod_1(n+h_c))}{(prod_2(n+h_c) - prod_1(n+h_c))} \cdot dF_r \cdot sign(cons\_prod(n) - prod(n)) \quad \text{(III.5)}$$

After verification of constraints respect, this radiant flux value F_r is applied to the process (to the level 0).

As the system is non linear, the production that would be obtained at time $n+h_c$ on the model with a radiant flux protocol equal to F_r is certainly different from $prod\_ref(n+h_c)$. It is then possible to iterate the procedure.

In the first version of the control law, this iteration has not been done. The experimental results will show if it is sufficient, or not.

Internal model

As an internal model, we could have chosen the complete knowledge model developped by LGCB (ref. Cornet TN19.1, 19.2, 19.3) but in fact, we have chosen to take just a part of this model.

This complete model is composed of 9 differential equations (9 states) those equations are the conservation equations for 9 main compounds in the reactor.

$$\frac{dC_i}{dt} = Dil \cdot (C_{E\text{-}i} - C_i) + \langle r_i \rangle \quad \text{(III.6)}$$

Dil is the dilution rate (Dil = q_e / vol) (vol is the reactor volume)

$C_{E\text{-}i}$ are the concentrations of the 9 compounds in the incoming flow.

C_i are the 9 concentrations in the reactor.

$\langle r_i \rangle$ is the mean growth rate for the different compounds.

As the mean growth rate of active biomass $\langle r_{xA} \rangle$ depends only on the biomass concentration C_{XA} and on the radiant flux F_r (in the case where the mineral limitations are not considered), we can define a simplified model, dealing only with the active biomass (a one state model).

If we add the mineral limitation problem in the continuation of the study, it will be necessary to complete the model with other compounds.

Model integration and initialisation

The internal model is caracterised by a non linear differential equation. We can choose different integration method.

In the first version of the control algorithm, the simplest integration method has been chosen : the Euler Method. It will be tested on the process.

The model integration is done from current time n to coïncidence time $n+h_c$. The initialisation of the model state is done with the measure of the biomass concentration. The advantage of a one state model is in the adaptation of the model state. This adaptation is obvious because the model state is measured. It's not necessary to use an estimation procedure.

III.4 - Level 2

This level concerns the "optimisation of setpoints", with respect to constraints.

The level 2 is supposed to receive a nominal production setpoint and a nominal flow value. The biomass concentration is limited by a minimal and a maximal constraint. The flow is supposed to be able to vary of dq_e % from the nominal value.

Then, with the constraints on biomass concentration, and the constraints on flow, it is possible to define a maximal and a minimal constraint on the production (eq III.9 and III.10).

The aim of level 2 is to modify, if necessary, the production and flow setpoints in order to respect the constraints.

The algorithm is described in paragraph III.5 (functional analysis of the control algorithm).

III.5 - Functional analysis of the control algorithm

- control period : dt = 1/2 hour
- 2 hierarchical levels

Level 2 : Optimisation of setpoints, with respect to concentration constraints

. *input :*

. nominal production setpoint : cons_prod_nom(n) (in g/h)
. nominal flow : q_e_nom(n) (in l/h)

. *output :*

. calculated production setpoint : cons_prod(n) (in g/h)
. calculated flow : $q_e(n)$ (in l/h)

. *parameters :*

. maximal constraint on concentration C_{XA}_max (in g/l)
. minimal constraint on concentration C_{XA}_min (in g/l)
. maximal variation of flow dq_e (in %)

. *algorithm :*

* determination of the production setpoint, to respect the constraints :

. maximal flow

$$q_e\_max(n) = q_e(n) \,.\, (1 + dq_e) \qquad \text{(III.7)}$$

. minimal flow

$$q_e\_min(n) = q_e(n) \,.\, (1 - dq_e) \qquad \text{(III.8)}$$

. maximal production

$$prod\_max(n) = q_e\_max(n) \,.\, C_{XA}\_max \qquad \text{(III.9)}$$

. minimal production

$$prod\_min(n) = q_e\_min(n) \,.\, C_{XA}\_min \qquad \text{(III.10)}$$

. production setpoint (respect of constraints)

$$cons\_prod(n) = \max(prod\_min(n), \min(prod\_max(n), cons\_prod\_nom(n))) \qquad \text{(III.11)}$$

* determination of the optimal flow :

if (cons_prod(n) . $C_{XA}\_max > q_e\_nom(n)$), then

$$q_e(n) = \min(q_e\_max(n), cons\_prod(n) / C_{XA}\_max) \qquad \text{(III.12)}$$

else if

(cons_prod(n) . $C_{XA}\_min < q_e\_nom(n)$), then

$$q_e(n) = \min(q_e\_max(n), cons\_prod(n) / C_{XA}\_max) \qquad \text{(III.13)}$$

else $q_e(n) = q_e\_nom(n)$ (III.14)

Level 1 : Control of the production, taking into account the flow

. *input :*

. biomass production setpoint : cons_prod(n) (in g/h)
. flow : $q_e(n)$ (in l/h)
. measure of biomass concentration : $C_{XA}(n)$ (in g/l)

. *output :*

. radiant flux : $F_r(n)$ (in W/m^2)

. *parameters :*

. λ : dynamics of the reference trajectory

$$\left(\lambda = \exp\left(- \frac{3\ dt}{TR} \right)\right)$$

TR : time response of the reference trajectory (desired closed loop time response)

. h_c : coïncidence point (in h)

. dF_r : increment of flux for the second scenario (in W/m^2)

. F_r_max : maximal constraint on F_r (in W/m^2)

. F_r_min : minimal constraint on F_r (in W/m^2)

IV - SIMULATION RESULTS

Tests in simulation are very important to evaluate the control method, its tuning and its robustness.

As the process is non linear, it is not easy to determine a priori the stability margins. So, the only way to evaluate the robustness is to test the control algorithm on the simulator in different functioning conditions.

IV.1 - Parameters tunings

- *Control period*

dt = 0.5 hour

This period is sufficient for such a system, and it allows to calculate a good estimation of biomass concentration.

- *Closed loop time response*

TR = 5 hours

which gives $\lambda = \exp(- 3 . dt/TR) = 0.75$

- *Coïncidence point*

h_c = 2.5 hours (nhc = 5 (. dt))

Those parameters are the main tuning parameters of the control algorithm. They define the dynamic of the closed loop.

Other parameters are defining the constraints on the radiant flux F_r, on the concentration C_{XA}, and the percentage variation on the flow (F_r_min, F_r_max, C_{XA}_min, C_{XA}_max, dq_e).

The last parameters are defining the model

zpc, zch, zg, Ea, Es, RT, Kj, muM, wiv,

It is a list of physical parameters of the knowledge model.

jstep corresponds to the step used in the calculation of the mean growth rate.

The radiant flux increment dF_r has been chosen constant. In a future version, it could be function of the difference between the production and its setpoint, if necessary.

All the parameters values that have been used in the different simulations are in the file comnl.h *(Annex B).*

IV.2 - Simulation results

Some tests of step on the production setpoint have been done at different dilution rate. There are increasing step and decreasing step.

The results are described on figures 5 to 10.

On the first graph, the nominal setpoint of biomass poduction (- -), the real setpoint (defined by the level 2 (- .), and the real production (-) are represented. They are all in g/h.

On the second graph, the radiant flux applied on the process is represented in W/m^2.

On the third graph, the biomass concentration and its constraints (- -) are represented in g/l.

On the fourth graph, the nominal flow (- -) and the real flow (-) defined by the level 2 are represented in l/h.

On all the tests, an added noise has been supposed on the measure of biomass concentration. It is a white noise of amplitude 0.025 *(figure 4).*

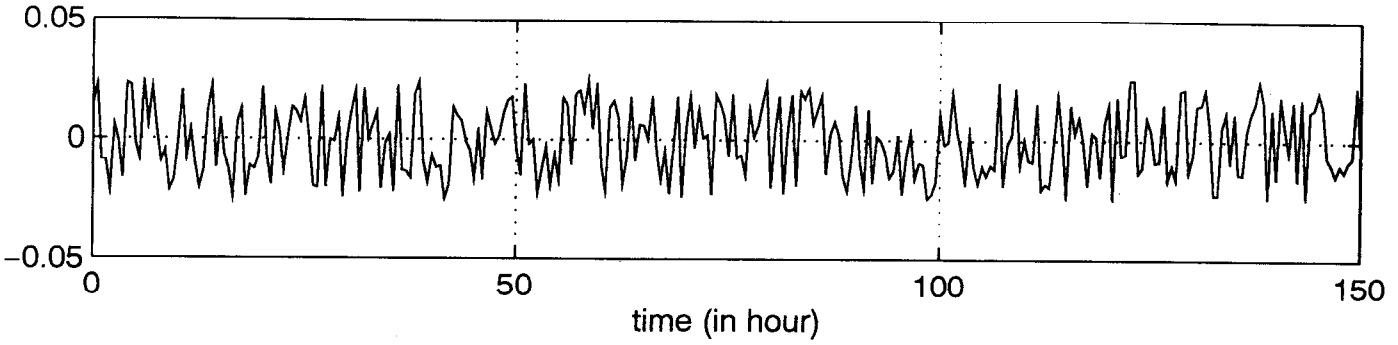

Figure 4 : Noise added on the concentration measure (in g/l)

- *First test (figure 5)*

The dilution rate is equal to 0.01 h^{-1}, the step of production setpoint is from 0.065 g/h to 0.09 g/h ; the constraints on biomass concentration are not reached. When the production setpoint changes, the maximal constraint on radiant flux is reached. The dynamic is limited by the constraint of radiant flux. For an encreasing step, it takes 10 hours to reach the setpoint.

- *Second test (figure 6)*

This test has been done with the same dilution rate (0.01 h^{-1}) but the step of production setpoint is decreasing from .09 g/h to 0.065 g/h. At that time, the radiant flux is on its minimum constraint ; the dynamic of the closed loop is then given by the dilution phenomenon. It is not the same dynamic as for an encreasing step. It takes 60 hours to reach the setpoint.

- *Third test (figure 7)*

The dilution rate is higher (0.02 h^{-1}). The behaviour is the same as on figure 5.

- *Fourth test (figure 8)*

This test is realized at a lower dilution rate (0.005 h^{-1}). The increasing step of biomass production setpoint forces the biomass concentration to its maximal constraint. Then the level 2 increases the flow (of 10 %) and decreases the setpoint.

The dilution rate is equal to 0.005 h^{-1}. The nominal production is equal to 0.06 g/h at time 50 hours, which would correspond to a concentration of 1.7 g/l (vol = 7 l). As the maximal constraint on biomass concentration is equal to 1.5 g/l, level 2 calculates a new value of production setpoint (equal to the product of the maximal constraint on biomass concentration with the maximal flow). This new value of production setpoint is equal to 0.058 g/l, it is represented on the first graph of figure 8. A new value of flow, which corresponds to an encrease of 10 % of the nominal flow is calculated too. It is equal to 0.0385 l/h, and represented on the fourth graph of figure 8.

- *Fifth test (figure 9)*

On this test, a variation of production setpoint and a variation of dilution rate can be found. The different constraints are reached so the level 2 modifies the flow and the production setpoint when it is necessary.

At time 50 hours, the nominal production setpoint is equal to 0.08 g/h. With a flow equal to 0.042 l/h, it would correspond to a concentration equal to 1.9 g/l. So, the level 2 calculates a new production setpoint equal to 0.069 g/h, which corresponds to a concentration of 1.5 g/l, and a flow increased of 10 %.

At time 100 hours, the nominal flow is increased to 0.049 l/h. But it is not sufficient to respect the constraint on biomass concentration. So, the level 2 calcultes a new value of flow (equal to the biomass production setpoint divided by the maximal constraint on concentration (0.08/1.5 = 0.053 l/h).

- *Sixth test (figure 10)*

On this last test, there is also a variation of dilution rate but at a higher value. The results obtained shows a great sensitivity to the noise measurement. It is due to the fact that the production is the product of the concentration with the flow. The noise been applied on the measured concentration, it is multiplied by the flow value. So the noise on the production estimation is proportional to the flow (or to the dilution rate).

IV.3 - Conclusion

The results obtained in simulation, on the Simulink non linear simulator (based on Cornet's model) are satisfactory.

This control law has to be tested on the real MELISSA process. This will be done in January 1995. In function of the experimental results it will be possible to change the tuning.

The implementation of the control law on the real process will be done on a PC. The programms (in C. language) are presented in Annex B.

It will be tested for different dilution rate, and different production setpoint, chosen in the validity domain of the process. For example, tests corresponding to figure 5 to 10 can be realized.

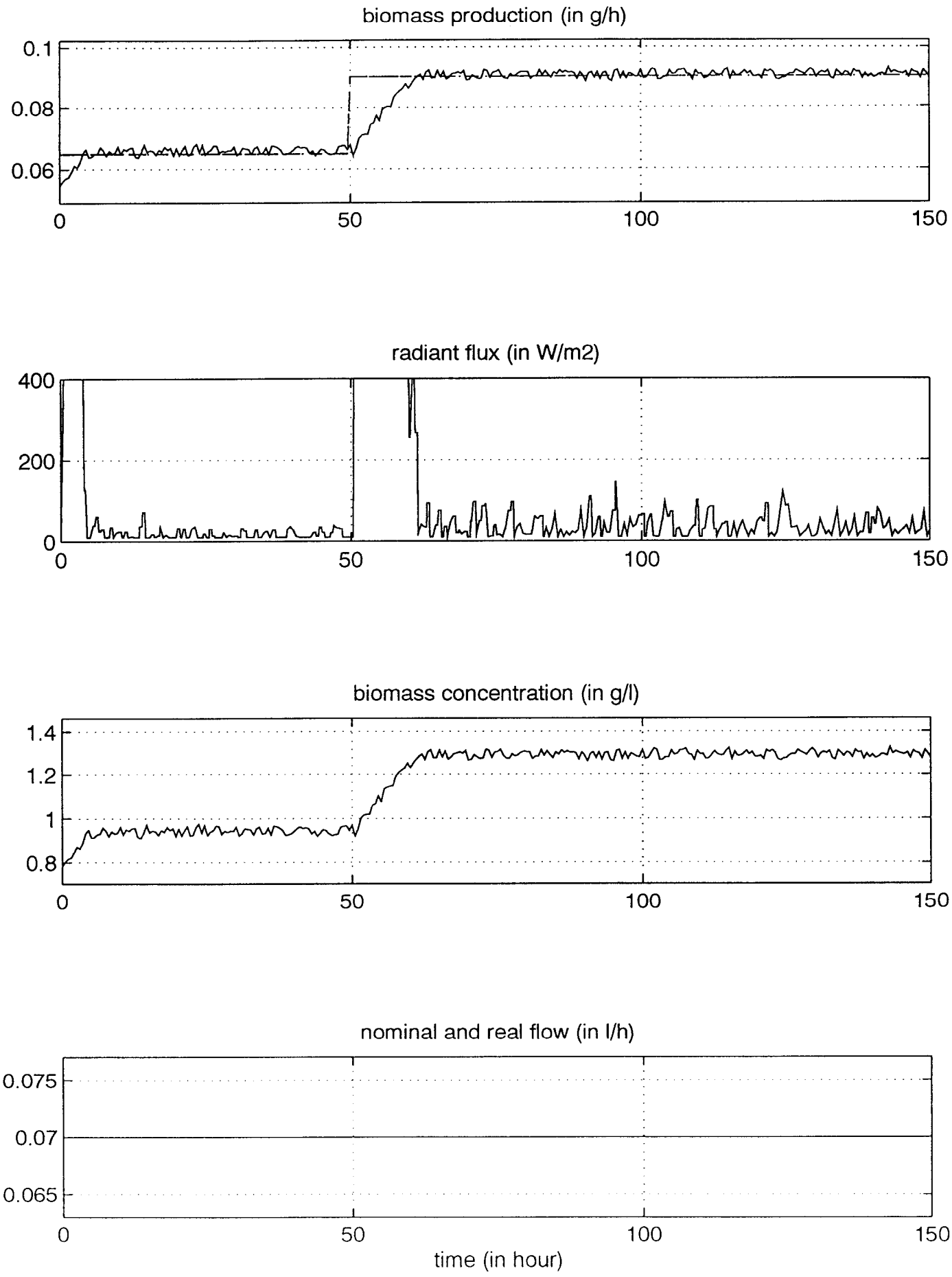

figure 5 : dil = .01 (1/h)

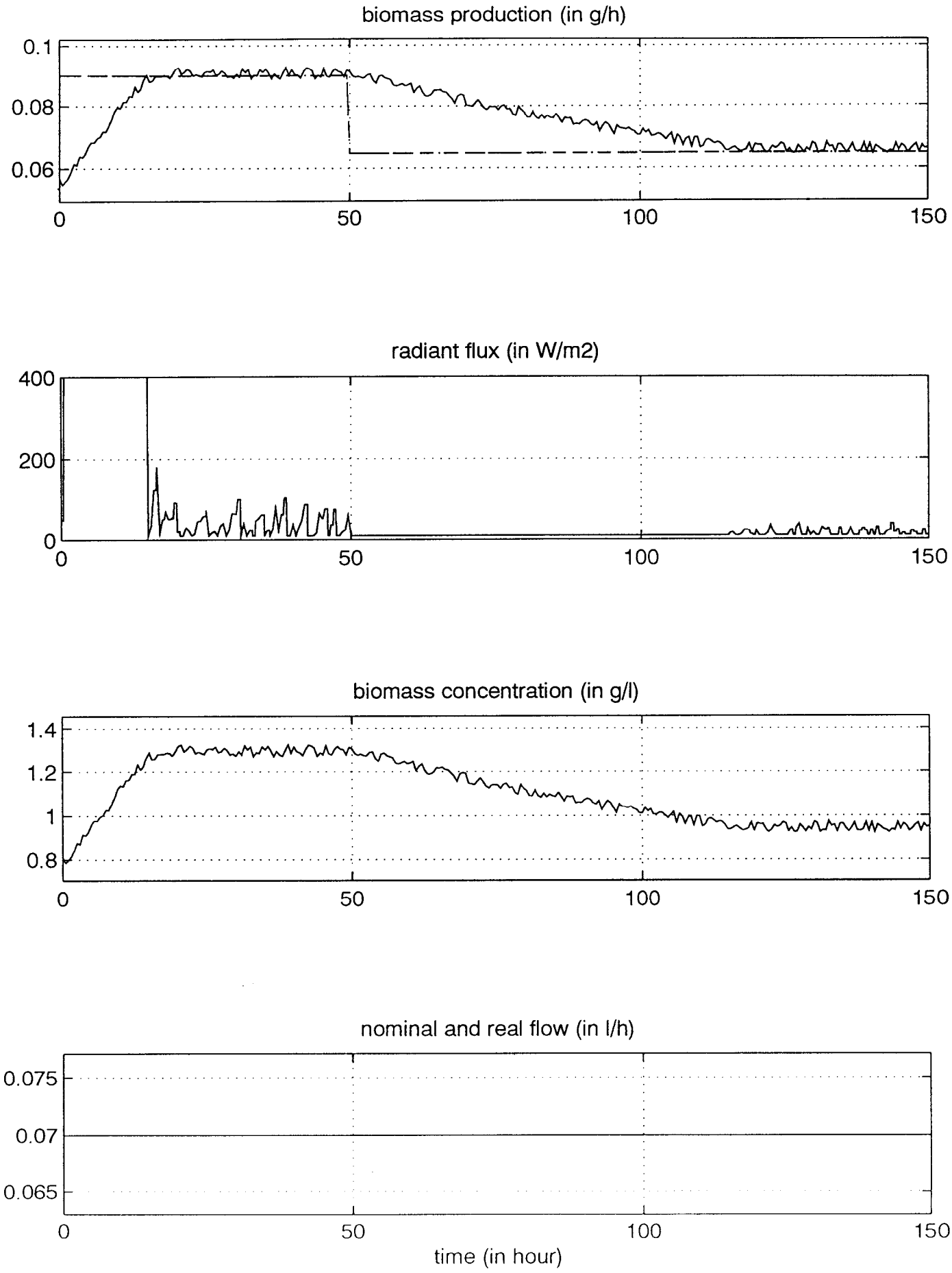

figure 6 : dil = .01 (1/h)

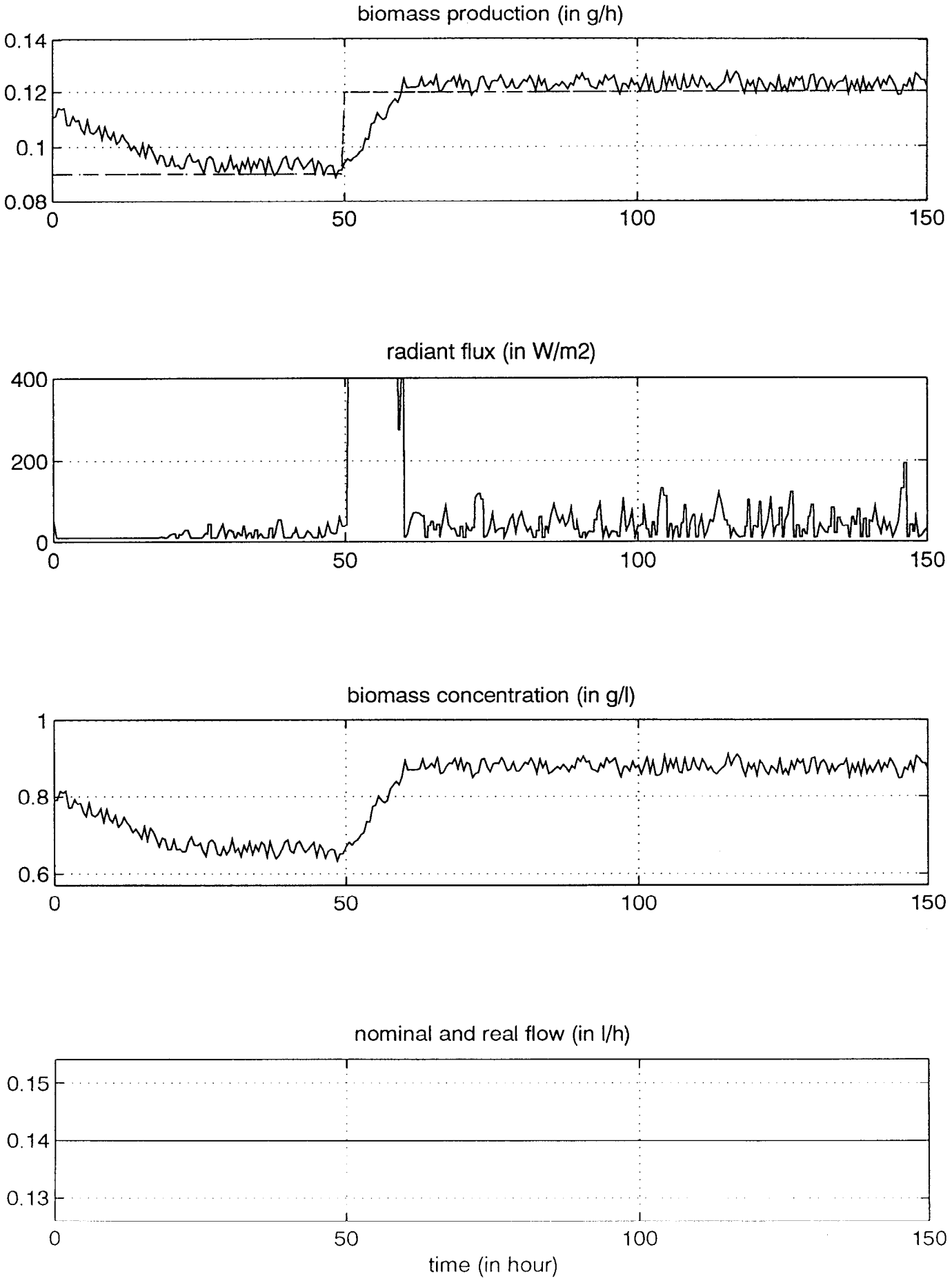

figure 7 : dil = .02 (1/h)

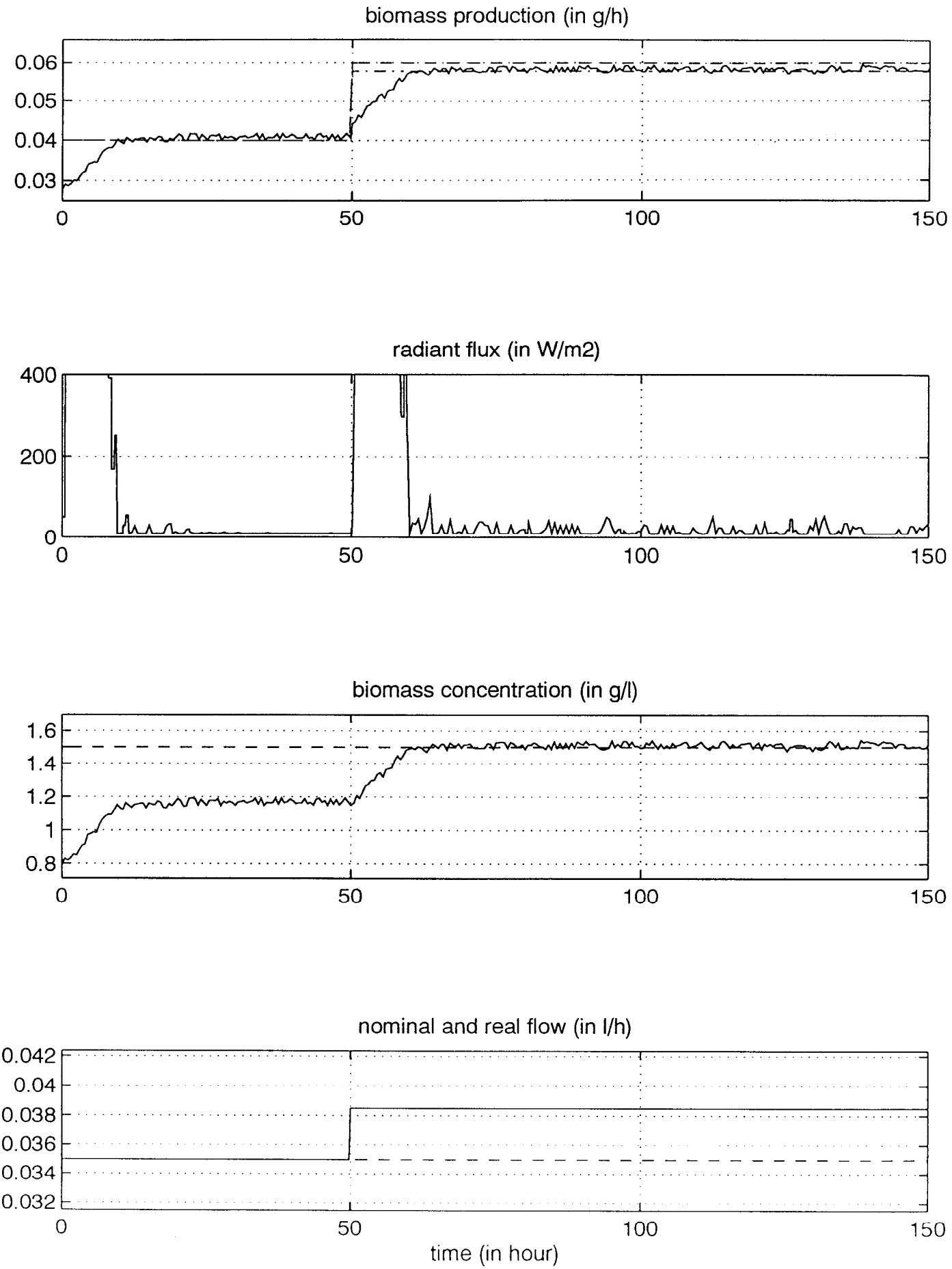

figure 8 : dil = .005 (1/h)

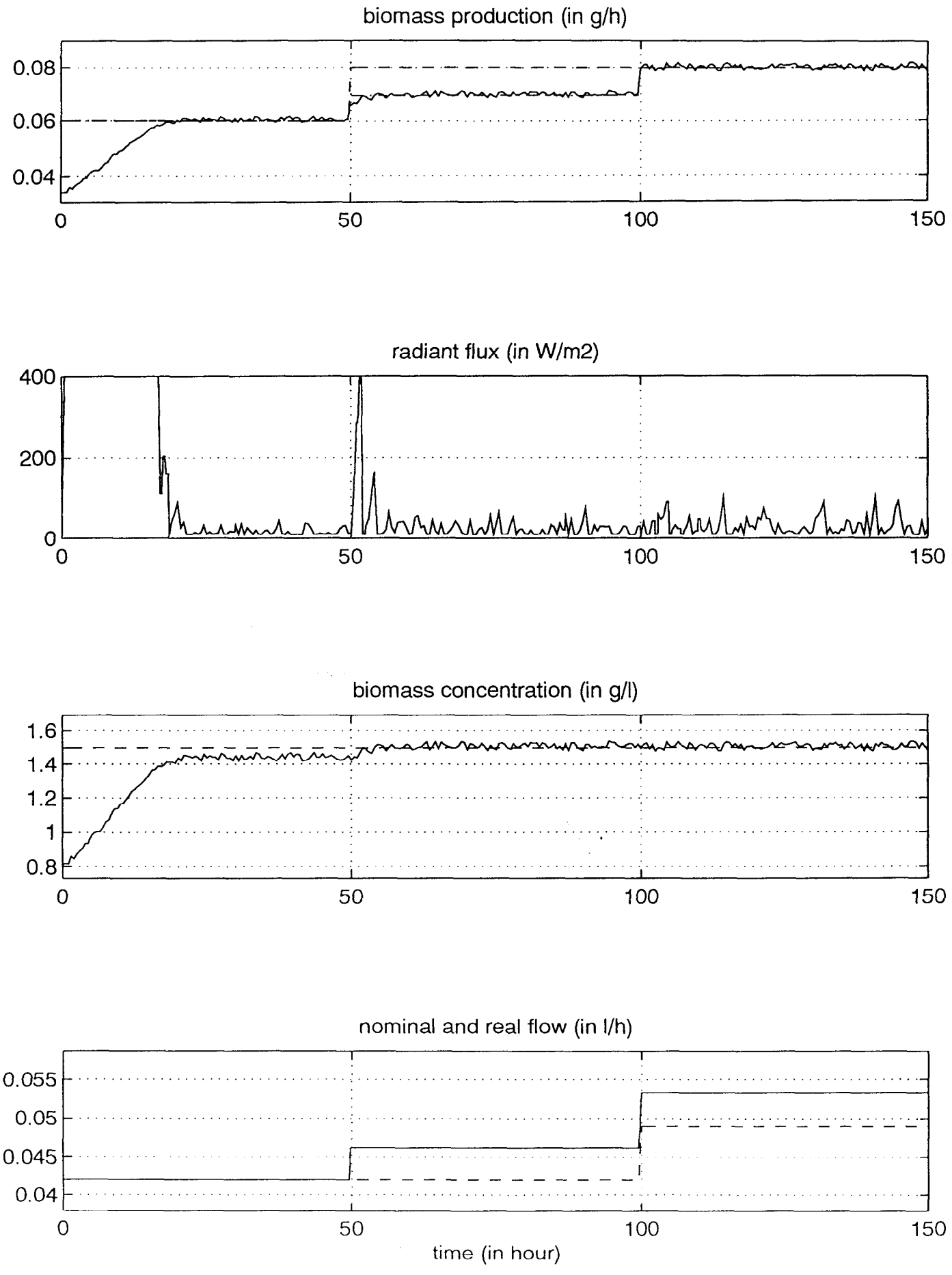

figure 9 : dil = .006 to .007 (1/h)

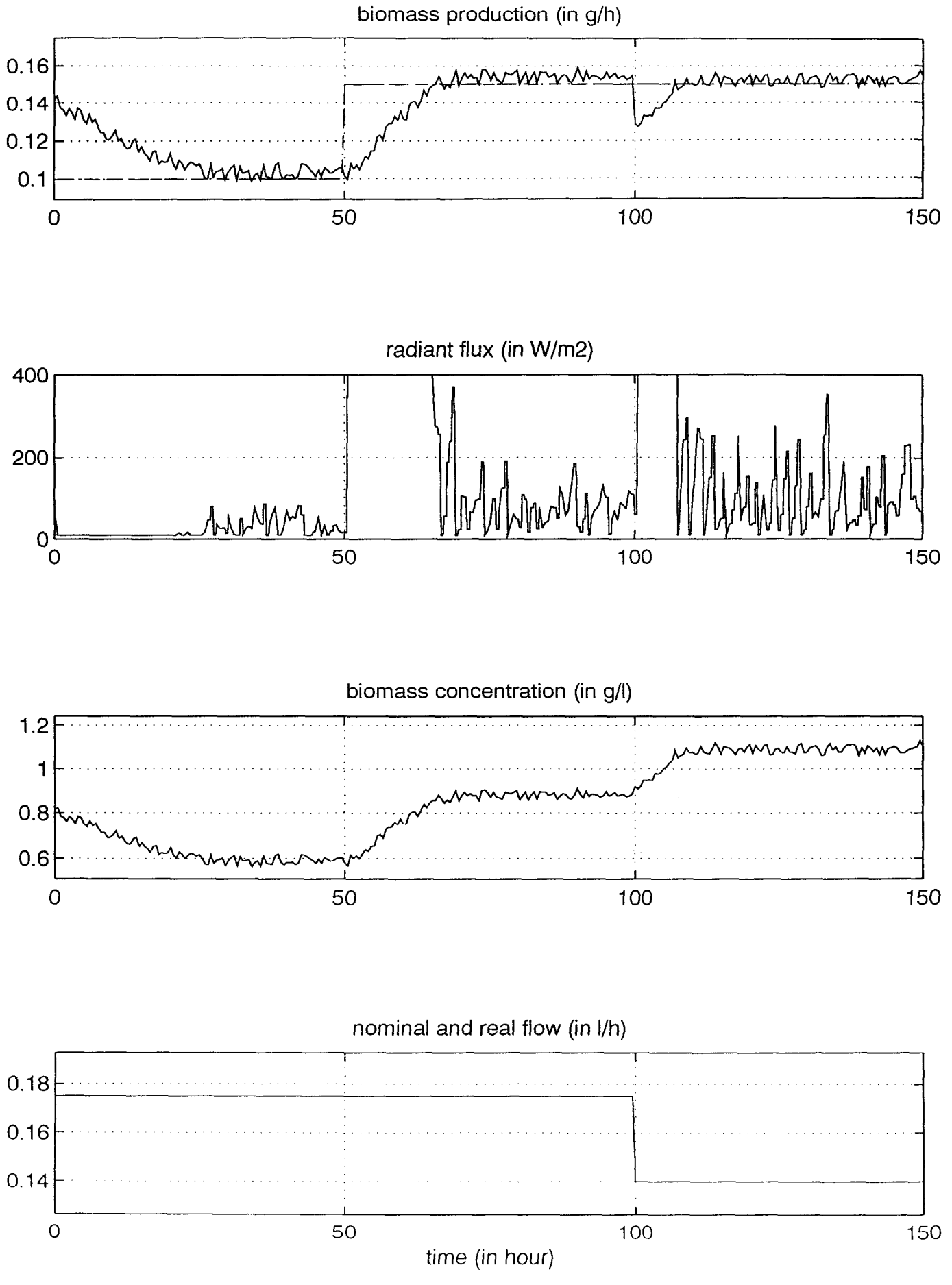

figure 10 : dil = .025 to .02 (1/h)

REFERENCES

BINOIS C. Automatisation d'un écosystème artificiel utilisé comme système de support vie. Première intéraction modèle/système de contrôle. CNAM Thesis. September 1994.

CORNET J.-F., DUSSAP C.G., GROS J.-B., 1993a. Modelling of physical limitations in photobioreactors. Adaptation of the light energy transfer model to cylindrical geometries. ESA contract PRF 130-820, Technical Note 19.1.

CORNET J.-F., DUSSAF C.G., GROS J.-B., 1993b. Modelling of physical limitations in photobioreactors. Modelling of exopolysaccharide synthesis in cultures of *Spirulina platenis*. ESA contract PRF 130-820, Technical Note 19.2.

CORNET J.-F., DUSSAF C.G., GROS J.-B., 1993c. Modelling of physical limitations in photobioreactors. Applications to simulation and control of the Spirulina Compartment of the MELISSA artifical ecosystem. ESA contract PRF 130-820, Tecnical Note 19.3.

FULGET N., 1994. MELISSA, first approach of Model Based Predictive Control of Spirulina compartment. ESA contract PRF 132-443, Technical Note 21.2.

RICHALET J., 1993. Pratique de la Commande Prédictive. HERMES Edition.

THAUVOYE O., 1994. MELISSA, Validation d'un modèle mathématique de croissance de bactéries photosynthétiques en photobioréacteur cylindrique. ESA report.

ANNEX A

- Industrial Application of Predictive Functional Control to rolling mill, fast robot, river dam

  The application to river dam has used the same strategy as the one used or MELISSA : "Scenario strategy"

Industrial applications of Predictive Functional Control to rolling mill, fast robot, river dam

J.M. Compas (Compagnie Nationale du Rhône)
P. Decarreau (Pechiney-Rhenalu)
G. Lanquetin (SEPRO)
J.L. Estival, N. Fulget, R. Martin, J. Richalet (ADERSA)

ADERSA - 7 bd du Maréchal Juin - BP 52
91371 VERRIERES-LE-BUISSON Cedex

ABSTRACT

After a brief presentation of PFC (Predictive Functional Control), 3 applications are described. Thickness control of a cold rolling mill, water level control of the Rhône river, and position control of a fast robot. The paper insists on the procedure : how to implement PFC and what can be expected from this technology.

1 - PREDICTIVE FUNCTIONAL CONTROL (PFC)

The principles of PFC were established in 1968 and the first applications took place in the early 70's. From that time on improvements were made possible, as they arose from the numerous problems that always emerge when any methodology meets true industrial applications.

PFC belongs to the classical family of Model Based Predictive Control since it fulfills the following 4 basic generic principles :

a) Internal Model : used for prediction
b) Reference trajectory : to specify the future closed loop behaviour
c) Structured future manipulated variable and algorithmic solver
d) Modelling error compensation to take into account prediction error.

a) Internal model

Any model can be used by PFC which is not limited to the ARMA representation. In fact, due to their robustness caracteristics, state space models are used most of the time. The model is called "independent" because it is only fed by the known manipulated variable MV (fig 1.1).

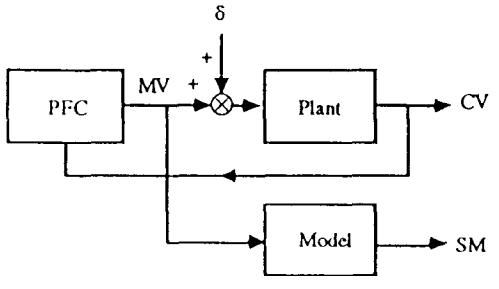

Figure 1.1 - Independent model approach
MV : manipulated variable, CV : controlled variable, SM : output of model

In case of underdamped modes or unstable systems, the decomposition principle allows the use of a stable internal model (M1), with the process output as a feed-forward variable through a stable model (M2). With such a procedure the disadvantages of the independent model approach are eliminated while its flexibility and efficiency are appreciated.

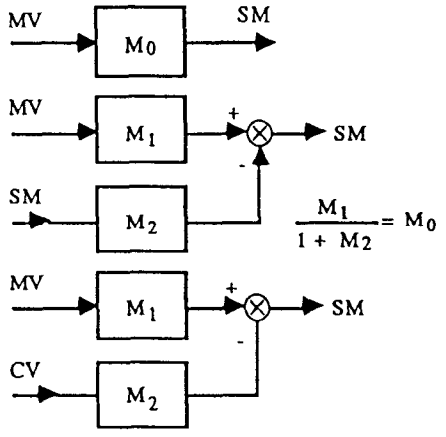

Figure 1.2 - Decomposition principle

b) Reference trajectory

It appears to be a direct and convenient way to specify the dynamics of the closed loop behaviour. It connects the measured or estimated controlled variable CV(n) to the future setpoint. A simple exponential trajectory ($\varepsilon(n+H) = \lambda^H . \varepsilon(n)$) is used over a receding horizon H_1 H_2 (figure 1.3).

Δ = Model output SM(n + H) - SM(n)
physical (Free Mode + Forced Mode)
specification

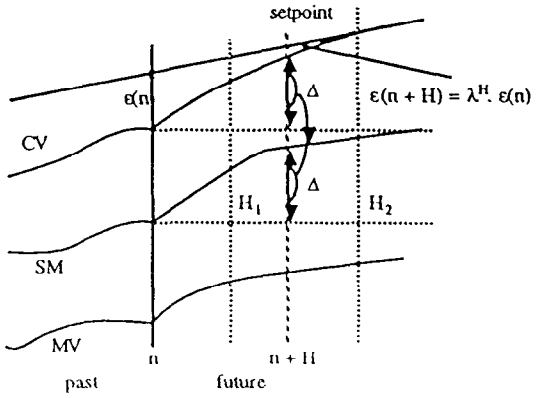

Figure 1.3 - Reference trajectory
H_1 H_2 : coincidence horizon

On normal well-behaved processes, a short horizon (e.g. $H_2 < 10\ T_S$ where T_S = sampling period) yields a smooth controlled variable (CV) and an active manipulated variable (MV). A far-away horizon ($H_2 > 15\ T_S$) is equivalent to mean value static control with a closed loop behaviour similar to the open loop behaviour of the plant but with a smooth MV.

c) Structured MV

Instead of looking for H_2 - 1 future MVs, with no restriction and problems attached (wild MV's which necessitate an a posteriori damping), it appeared easier to structure future MV's by :

$$MV(n+i) = \sum_K \mu_K UB_K(i) \rightarrow \text{Forced solution} = \sum_K \mu_K SB_K(i) \quad (1)$$

where $UB_K(i)$ belongs to a set of base functions (figure 1.4) which can be, for instance, a limited Taylor expansion.

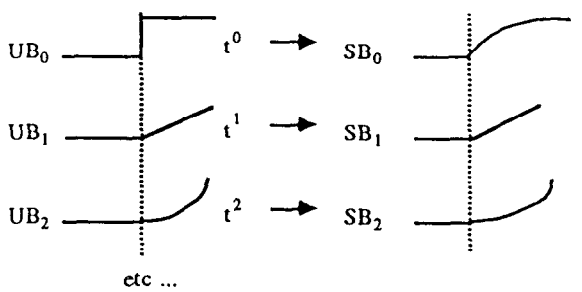

Figure 1.4 - Polynomial base functions

The selection of the base functions is driven by considerations on the nature of the setpoint and the integrative nature of the process. If the assumed future setpoint (known or estimated), is an eigen-function of the known process (polynomial or harmonic) then by selecting accordingly the base functions, one can demonstrate that in the nominal case (model = process) there will be no lag-error on any setpoint (fig 1.5).

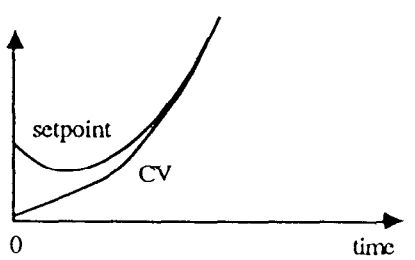

Figure 1.5 - No lag-error on polynomial setpoint

A pseudo-inverse solver over H_1 H_2 turns out to give an equivalent linear controller acting on setpoint, feed back signal, and error.

d) Modelling error

Either state additive perturbations or structural perturbations (model mismatch) affect the model output which is always different from the process output. Several procedures can be used to take into account the predicted error at time n + H ($H_1 \leq H \leq H_2$). One of them is to use a polynomial least square estimate of $e_M(n)$ to predict the error, and therefore, modify the reference trajectory at time n + H and thus eliminate a possible permanent off-set (figure 1.6).

An harmonic estimator can be used as well to eradicate sinusoidal perturbations at a prescribed frequency ω_0 (see the "hill curve" of figure 1.7).

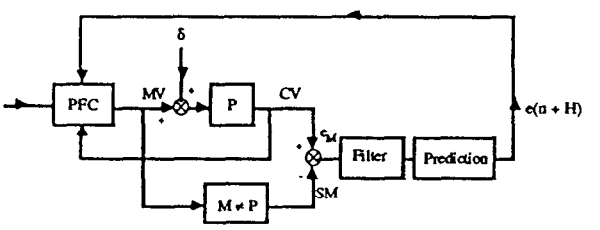

Figure 1.6 - Error compensation procedure

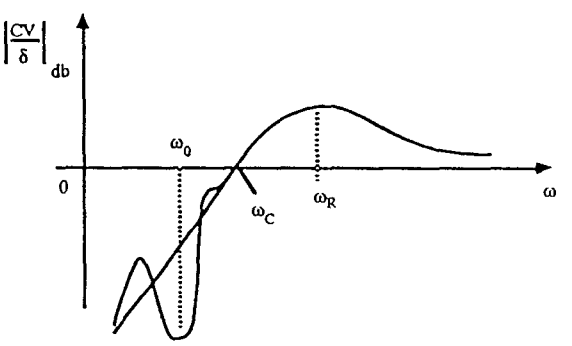

Figure 1.7 - The "hill curve" with harmonic compensator at $\omega = \omega_0$

e) Constraints

Supported by a long proved field experience PFC is nowadays a standard in some fields (defence). When constraints, either on MVs or CVs have to be taken into account, PFC has a definite advantage over non predictive methods. Let us cite D. Clarke. "Thinking men suggested that infinite-horizon LQ was the answer, but this involved the loss of ability to solve the important problem of constraints ... . It is the incorporation of inequality constraints on actuator or state variables which uniquely gives MBPC its power, for then the plant can safely be driven closer to its ultimate operating limits" [2] [4]. Let us note that infinite horizon approaches present valuable theoretical results and that finite receding horizon approaches correspond to the practical industrial need to locate the state vector, in a finite time, within the constrained domain of actions. Constraints on CVs are partially treated by a classical logical procedure :

"the multiple controller approach", similar to over-ride [1]. The constraints become the set-points of constrained controlled processes and a supervisor selects, according to a full prediction in future time, the MV, among MV_1 and MV_2, which is compatible with setpoint and constraint specifications (figure 1.8).

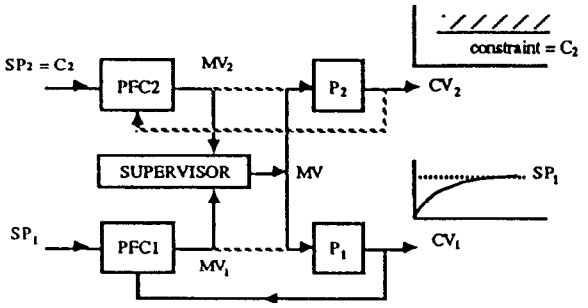

Figure 1.8 - Control of CV_1 subject to constraint on CV_2

f) Field of application

- defence : follow-up servos with no lag error : pointers, gun-sight, laser director, antennas, radar, video, missile launch, camera-mount, gun pedestal, missile auto-pilot, etc ...
- chemical batch reactor with non-minimum phase effect and exothermic reactions, follow-up time varying recipes, etc ...
- flexible mechanical systems with many underdamped modes, measuring systems, etc ...
- automotive : idle injection control, clutch control, richness control, active braking, suspension, temperature control, etc ...
- steel and aluminum industry : continuous casting level control, gas furnaces, pressure, pushing ovens, hot and cold rolling mills, etc, ...

Here we present 3 typical applications which are not classified and where some information can be partially disclosed.

Rolling mill : It is a comprehensive application which has been followed up with permanent improvements over 6 years. Thickness control and roll-excentricity compensation brought an interesting pay-back to be expressed in terms of weeks.

Fast robot : It is a full CAD application where the robot manufacturer completely changed its working procedure and aims now at a full Integrated Design approach.

River dam : It is a highly non-linear integrative control problem with hard constraints. A "first principles model" is used on-line.

In all these applications, the industrialists were aware that Advanced Control does not boil down to moving from PID to a new algorithm. It involves a different approach where modelling is the key issue.

2 - PREDICTIVE CONTROL OF COLD ALUMINIUM ROLLING MILLS

2.1 - Introduction - Why Advanced Control ?

Every second 500 aluminium beverage cans are manufactured throughout the world. The average weight of the Coca-Cola type can is nowadays around 15 g, while it was around 30 g in 1970. It is a highly competitive expanding market, gaining shares on steel cans. To comfort its position Pechiney International, the leader in canning, was compelled to use high-tech control techniques. Variance of thickness has been permanently decreasing while productivity (rolling speed) has been increasing. Accuracy may appear abusively high for such a common or vulgar product : thickness of the input strip is around 750 µm at the front end of the rolling stand while the standard deviation of thickness at the output end is around 0,5 µm ! The classical "give-away scheme" : 2S's. "Squeeze the variance - Shift the set-point" is applied to full extent and any gain on thickness accuracy is used to decrease the weight of the can. The marginal gain of canning companies, being of the order of magnitude of the cost of scrap material, any progress on thickness is appreciated.

The rolling stand is a very much disturbed unit : high speed rolling (> 1800 m/min) induces a thermal ramping perturbation that cannot be controlled in a robust way by ordinary PID control techniques or by any technique unable to take constraints into account. The plant is highly non-stationary and, if no end cut-off of strips is a target (to maximize productivity), a time varying internal model is necessary whereas an ordinary set of adapted gain scheduled controllers is almost impossible to maintain (fig. 2.1, 2.2).

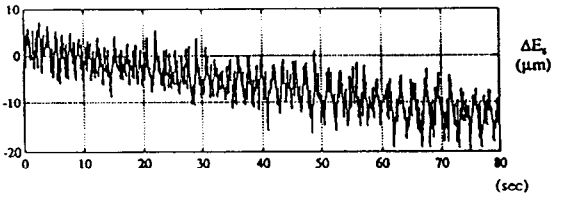

Figure 2.1 - Thermal drift (open loop)

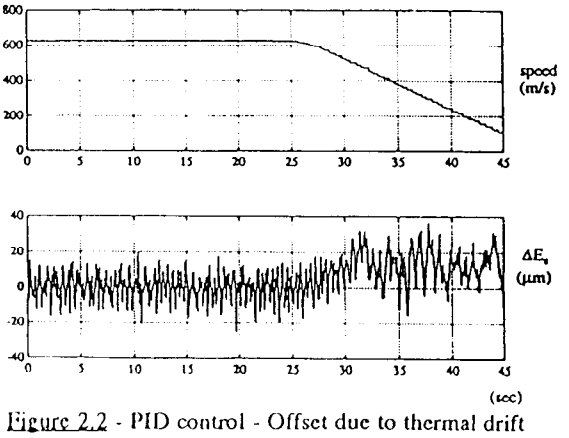

Figure 2.2 - PID control - Offset due to thermal drift

To avoid a "witch-tuning" approach, a more professional, i.e. model based and predictive method seemed more reliable. Moreover a responsible comprehensive study, from modelling to computer implementation, is more perennial than local academic tests.

A typical one-stand cold rolling mill is described by figure 2.3.

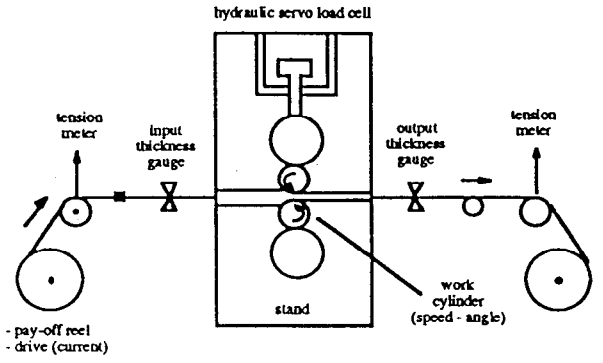

Figure 2.3 - Physical description of rolling mill

The useful variables are :

MV's	:	hydraulic pressure of load cell (or position of servo)
	:	speed of work cylinders
	:	current of pay-off reel drive
CV's	:	thickness of output strip
	:	flatness
	:	tension of pay-off reel
measured DV	:	input thickness of strip

Basic instrumentation is composed of 2 "Xrays" gauge sensors, 2 strip tensio-meters, speed and position of rolls sensors, diameter of reels, etc. Many perturbations affect the process.

State perturbations

Defects from up-stream rolling mills are printed in the input strip. The stand itself has many mechanical defects, if less than a micron accuracy is at stake, lumped under the term "roll excentricity". It is not a pertinent term because the alleged geometric unbalance is not at all the only source of disturbances. They come for bearings, supports, thermal deformation at high speed, etc. The stochastic environment is quite unstationary and a-priori geometric compensators are too limited.

Structural perturbations

The whole system is submitted to high forces (1000 T), torques, and massive energy transfers. Large power is dissipated in the stand and in the strip, generating unstationary disturbances that make control more complex and necessary. The process transfer function varies with speed, nature of alloy, thickness and width of strip at input, inertia and diameter of pay-off reel, flux of the electrical drives, etc. Acceleration and slow down affect largely the control system. The manufacturer himself is a source of perturbation since the market and materials vary quite often. Flexibility is becoming nowadays a key problem in the control strategy.

2.2 - Modelling

From the original reference of Bland and Fort (1948) many models were derived, some of them dynamic and identified on real data [7] [9] [10].

Black-box modelling is not sufficient and "first principles" models, though more costly and difficult to derive are necessary for the following reasons :

- control should be efficient during transient periods of rolling at varying speed if no strip ends cut-off is looked for ;
- a massive set of black-box models should be avoided if a good trade-off between robustness and dynamics is a target ;
- tuning is preferably done on an a-priori model, to avoid numerous and tedious costly local tunings.

However, the full model is quite large due to the complexity of the plant coming from interaction between the stand resilience, the pay-off reel inertia, the drives level 0 control and the strip elasticity. Since the sampling period is to be selected between 4 ms and 20 ms, no computer is available for such complex simulations in real time at a reasonable cost.

The first major work was thus to extract a simplified model and to derive a set of easier transfer functions linking MV's and CV's from the basic linearized assumption :

$$\Delta E_s = K_e \Delta E_e + KT_e \Delta T_e + KT_s \Delta T_s + KX \Delta X \quad (2)$$

where ΔE_s, ΔE_e are output and input thickness, ΔT_i tensions, ΔX the position of the hydraulic servo-valve and ΔC_e the braking torque.

$$\begin{vmatrix} \Delta E_s \\ \Delta T_e \end{vmatrix} = \frac{\begin{vmatrix} KX(1+\alpha s^2) & \frac{-KT_1}{k_1} & KE(1+k_2\tau s+\alpha s^2) \\ \frac{KX\,k_3}{KT_1} & \frac{1}{k_3} & \frac{KE}{KT_1}\tau s \end{vmatrix}}{1+\tau p+\alpha p^2} \begin{vmatrix} \Delta X \\ \Delta C_e \\ \Delta E_e \end{vmatrix} \quad (3)$$

where α and τ depend, through an analytic formula, on speed, Young modulus, input thickness and pay-off reel dimensions etc ...

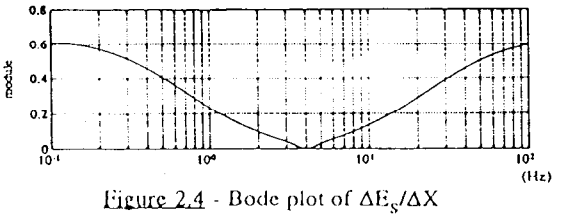

Figure 2.4 - Bode plot of $\Delta E_s/\Delta X$

The model is valid from 0 to 20 Hz if level 0 actuator and time delays of gauge are taken into account. The bode plot of transfer $\Delta E_s/\Delta X$ has a typical "bird wing" shape due to elasticity of strip between reel and stand. No perturbation around 4 Hz can be controlled by hydraulic pressure only (fig. 2.4). A large test signal campaign with adapted protocoles was designed so that after a limited number of learning trials, the procedure could be optimized and used during production. Like in many other situations PRBN test signals are to be avoided. Dedicated and deterministically optimized sets of wobulated steps are more efficient. Global identification techniques enable to work with a poor signal to noise ratio, give the model uncertainty and, most important of all, allow protocole optimization [12].

Figure (2.5) gives an example of the iso-distance domain D_0 in the parametric space KX, KT_1 ($D_0 = \Sigma\ (s_M(n) - sp(n))^2$) ($s_M$ = output of model, s_P = output of process).

Figure (2.6) gives an example of large test signals applied to model and process.

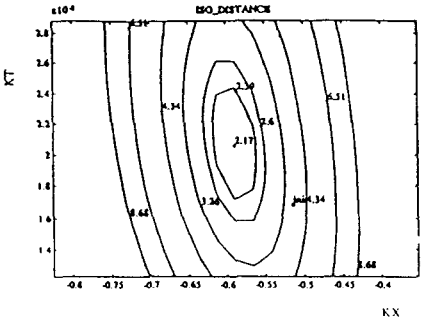

Figure 2.5 - Iso-distance parametric space KT, KX

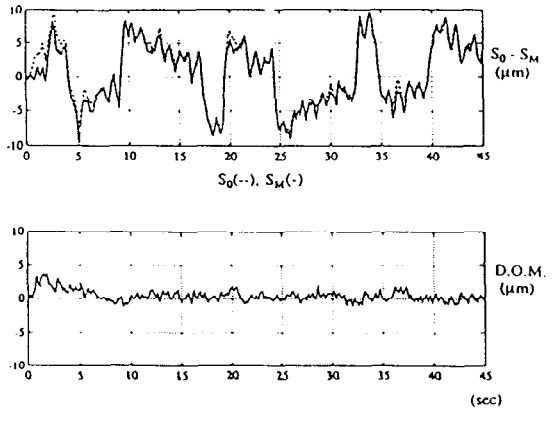

Figure 2.6 - Identification of transfer $\Delta E_s/\Delta X$

2.3 - Tuning PFC

2.3.1 - Model

The model is given in terms of discrete state variables with non-stationary parameters. It is simulated on-line and yields free mode and forced mode predicted outputs of model.

2.3.2 - Reference trajectory

Selected as an exponential, it specifies the closed loop time response selected at a constant ratio (close to 1) with the open loop time response that varies with speed. To respect robustness requirements such a tuning was finally adopted (fig. 2.7).

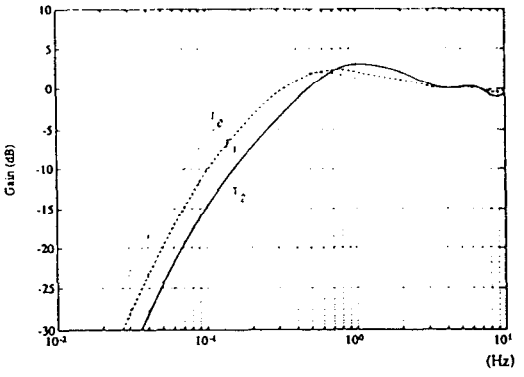

Figure 2.7 - Hill characteristics for 3 reference trajectories

2.3.3 - Base functions - Coincidence horizon

Ramp like perturbations impose the selection of 2 base functions : step and ramp function. Coincidence horizon was selected through PFC CAD package to optimize the position and magnitude of the "hill characteristics", the stability margin (gain margin, time delay margin) and the amplitude of error (fig. 2.8).

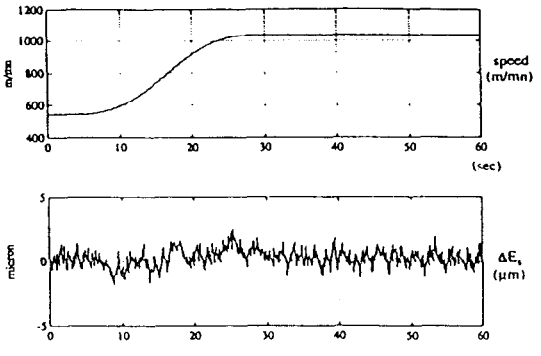

Figure 2.8 - PFC control at varying speed

Feed-forwarding the input thickness is done through models of level 0 and stand. A polynomial self-compensator is also used to exploit on-line the discrepancy between model output and process output during varying and permanent speed. No offset is then observed during transient periods (fig. 2.9).

Speed and absolute value constraints affect the different MV's and the input tension. Constraints appear to play a critical role.

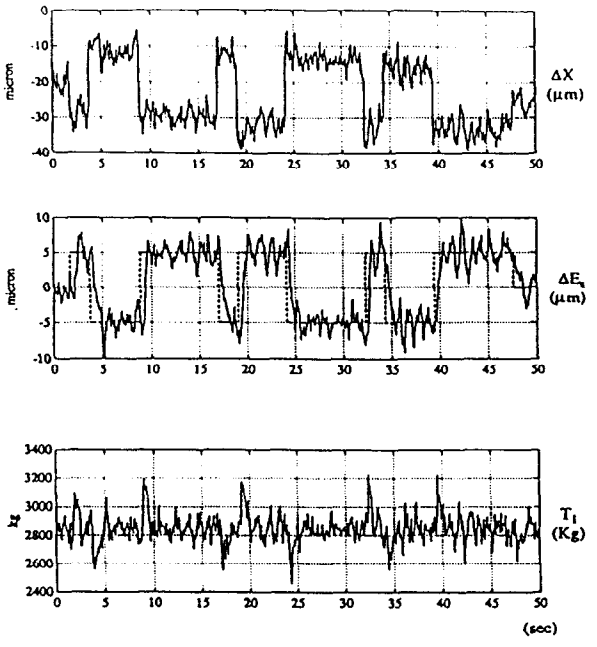

Figure 2.9 - PFC control - Setpoint change of ΔE_s at constant tension T_1

2.4 - Roll excentricity

Many techniques are proposed by several authors but geometric compensation and Fourier transformed based analysis are inappropriate in that case because of their long time response, since compensation is supposed to work at all speeds.

On-line recognition of the harmonic signal s(t) at frequency f_0 is obtained through an on-line identification procedure (at 4 ms sampling period).

$$s(t) = A \sin(2\pi f_0 t) + B \cos(2\pi f_0 t) \qquad (4)$$

which minimizes the Lyapounov function :

$$D(t) = (A_m(t) - A_p)^2 + (B_m(t) - B_p)^2 \qquad (5)$$

where A_m, B_m and A_p, B_p are the signatures of model and process signals.

4 frequencies with 3 harmonics coming from stand rolls (figure 2.10) are completely compensated by an extra PFC multivariable controller acting on hydraulic pressure and input tension.

2.5 - Results - Future work

Implemented in 1988, PFC has increased productivity by a factor 2 and reduced standard deviation by a factor 5, over classical PID control,.with almost no strip clipping. Permanent improvements were brought to the control system during the last 6 years (acceleration, supervision, etc).

Nowadays the variance is close to the asymptotic figure defined by the accuracy of the gauge. The target is now to "reduce the variance of the variance". The process exhibits structural perturbations due to lubrification, mechanical wear and strip characteristics. On-line identification of the basic parameters K_i is performed in the general frame of a supervision system. Supervision, per se, brings no pay-back if it is not considered as the elementary sensor of a Model Based Diagnosis procedure. The goal is to detect alterations of the stand, to ease maintenance but not to self-tune on-line the controller.

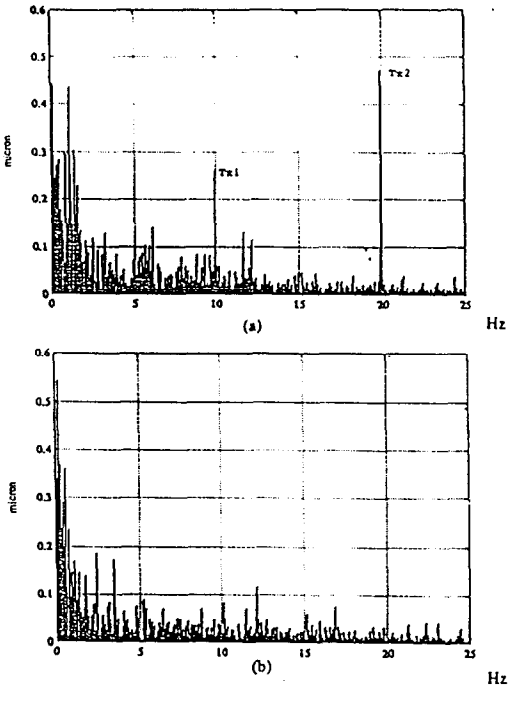

Figure 2.10 - Without (a) and with (b) roll excentricity compensation

Conclusion

Due to availability of reliable CAD packages (PFC Matlab, GLIDE Matlab), 90 % of the time could be spent on physical analysis, modelling and tuning of the simulator. The model appears now to be a valuable proprietary corporate stored know-how. From the permanently up-dated simulator, control and diagnosis procedures are derived and used by several services of the company.

Lack of perennity is a classical feature of Advanced Control attempts, if the simulator is not maintained. The model brings an objective knowledge independent of actors' ability or good will, but CAD packages need to be true professional tools to adapt rapidly to the varying market conditions.

3 - CONTROL OF A FAST AND ACCURATE ROBOT

3.1 - Introduction

If Advanced Control is a must on two-degree-of-freedom defence servomechanisms, most practical industrial robots do not need sophisticated

controllers. Rigid arms and large gear ratios, no follow-up specifications, help make this kind of process controllable by simple PI schemes (welding, pick and place ...).

The Sepro 450 family of robots is used for the manipulation of plastic parts coming out of extrusion machines and going through a well defined path to a piling up stack. Accuracy is to be less than 1 mm over a 1500 mn dynamic path and the docking accuracy should be less than 0.2 mn. Acceleration is limited to 20 m/s^2 and speed reaches 15 m/s. Load at wrist level may vary from 0 kg to 20 kg.Since the time for this transportation is in the production line time, it has to be decreased as much as possible to improve productivity.

The goal is two-fold :

- to achieve the above specifications with a 3-degree of freedom cartesian robot, with flexible modes and power constraints ;
- to ease the tuning of the controllers of the different robots that are customized for every different applications.

Improvements are demanded by the end-users but also by the manufacturer who wants to move towards a more systematic approach.

3.2 - Speed control - Position control

For industrial reasons the first 2 elements of the cascade of the 3 usual controllers : current, speed and position were kept unchanged (variator). The problem was then to apply PFC for position control through an MV now equal to the speed set point. The process can be modelled by the simplified scheme of figure (3.1). To eliminate the integrative effect, a feedback loop (gbpos), with a simple gain, was used. That procedure can be justified by the following reasons :

- test procedure is easier and more reliable with an asymptotic stable system ;
- input signals are composed of classical trapezoidal or triangular speed set point, respecting current (60 A) and power limitations. They properly excite the significant modes, at operating values close to their physical constraints ;
- industrial limitations (the 3 axis controllers should be on the same board) imposed limits on the computational load (T_s = 9 ms), and no error compensating procedure could be used. To remove ramp permanent error, an a-priori position loop thus appeared necessary.

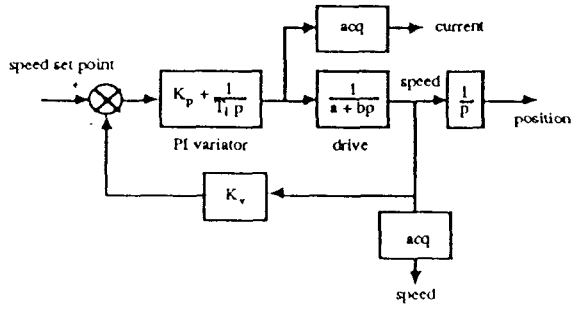

Figure 3.1 - Cascaded control

Tuning the position loop is easily done, since the process is equivalent to a pure integrator. If an open loop time response of 150 ms is looked for, then the equivalent time constant is close to 50 ms and the feed-back gain is :

$$gbpos = 20 = 1/0{,}05 \text{ sec}^{-1}$$

The PFC position controller may speed up the closed loop time response by a factor 2 or 3 without jeopardizing robustness, so that a 50 ms time response seems reachable (fig. 3.2).

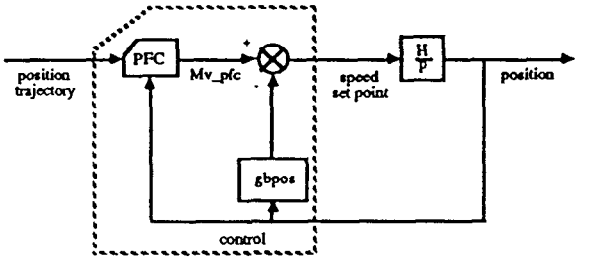

Figure 3.2 - PFC position controller

3.3 - Modelling

Modelling was done first in an open loop way (gbpos = 0), but afterwards in a closed loop way assuming the process to be a first order system. The protocol was triangular and figure 3.3.a shows an apparent perfect model, with no visible difference between model and process over 1,2 m. However an acute observation of the model error shows a flexible mode of magnitude ± 1 mm, too large for the specified accuracy. Introduction of a flexible mode in the transfer function :

$$\frac{\text{position}}{\text{Mv\_pfc}} = \frac{1/gbpos + b_1 s}{(1 + \tau s)\left(1 + \frac{2\xi}{\omega} s + \frac{s^2}{\omega^2}\right)} \qquad (6)$$

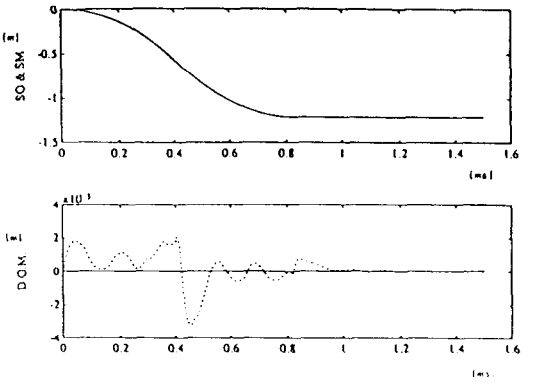

Figure 3.3.a - Open loop identification (1rst order model)
SO : process output - SM : model output - D.O.M : difference object-model

Global identification GLIDE gives for the different loads : τ = 48 ms for 0 load, τ = 53 ms for 25 kg load. The disensitizing effect of the position feed-back can be appreciated (fig. 3.3.b).

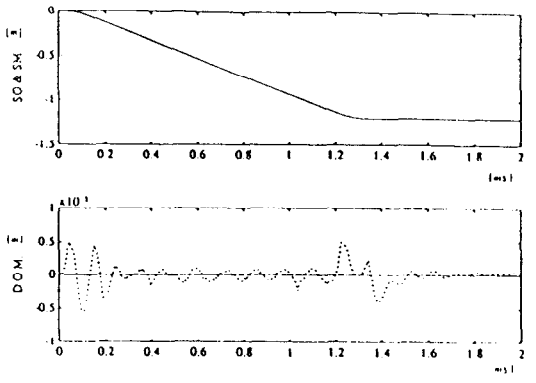

Figure 3.3.b - 3rd order model identification

Max, Min values of the parameters are given by table 1.

The oscillating mode is not well sensitized due to its small influence with respect to the other mode. No tuning of PFC will be feasible if the needs for robustness are not clearly specified. For trapezoidal protocols the pulsation varies from 70 rad s^{-1} for 0 load to 55 rad s^{-1} for 25 kg. Triangular protocols give slightly different values : e.g. average value 55 rad s^{-1} for trapeze, 48 rad s^{-1} for triangle. These uncertainties come from neglected non-linear effects, they will be taken into account during the robustness dynamics trade-off tuning of the controller.

	Pmod	Pmin	Pmax
τ(s)	51.8 e^{-3}	50.5 e^{-3}	53.3 e^{-3}
ω (rd s^{-1})	55	53	57
ξ	0.28	0.22	0.35
b_1 (s^2)	9.1 e^{-4}	7.6 e^{-4}	11.1 e^{-4}

(a)

	Pmod	Pmin	Pmax
τ(s)	47.9 e^{-3}	47.3 e^{-3}	48.6 e^{-3}
ω (rd s^{-1})	70	68	72
ξ	0.37	0.32	0.43
b_1 (s^2)	7.4 e^{-4}	6.4 e^{-4}	8.6 e^{-4}

(b)

Table 1 - Isodistance - model uncertainty (a) 24 kg, (b) 0 kg

3.4 - Tuning PFC

3.4.1 - Internal model

No adaptation with load being feasible only one internal model is used. Several models were tested with respect to robustness and finally the best trade-off was selected as a full load model with the linear model.

$$H = \frac{0{,}05 + b_1 s}{(1 + \tau s)\left(1 + \frac{2z}{\omega} s + \frac{s^2}{\omega^2}\right)} \qquad (7)$$

with : $b_1 = 1{,}2\ e^{-3}\ sec^2$
$\tau = 53\ e^{-3}$ sec
$\omega = 51$ rad/s
$z = 0{,}36$

3.4.2 - Decomposition of mode

The flexible mode frequency and damping vary in a large range. Decomposition (cf. 1) is used to shift the initial modes - 18 ± 47.towards τ_1 and τ_2, two real modes given by the tuning table 2 (fig. 3.4).

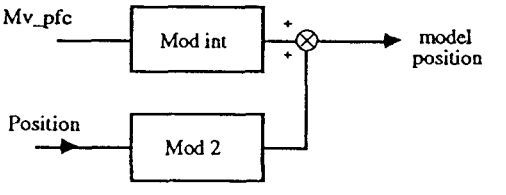

Figure 3.4 - Decomposition of flexible mode

τ_1, τ_2	decomposed modes
MG, MP, MR	gain, phase and time delay margins
TRBF	closed loop time response
DEP %	CV overshoot
U_{max}	MV_{max}
ET(y), ET(u)	standard deviation of CV and MV for a white output additive perturbation (gaussian noise σ = 1)
TRET	time response to initial off-set
Y_{max}	CV_{max}
FCC, FCP	cut-off and peak frequencies (Hz) of hill curve
$(Y/D)_{max}$	peak of hill curve
N(+), N(.)	number of add. and mul. operations

Decomposition

Tau1	Tau2		MG	MP	MR	TRBF	DEP %	Umax	ET(y)	ET(u)	TRET	Ymax	FCc	FCp	(Y/D)max	N(+)	N(*)
0.02703	0.02703	1	5.048	91.55	0.1122	0.063	0	95.3	0.41	215.8	0.171	1	8.741	2.369	1.314	14	16
0.01923	0.02703	2	4.278	88.93	0.02333	0.054	0	96.18	0.4853	266.1	0.144	1	9.746	10.87	1.395	14	16
0.01923	0.01923	3	3.741	72.32	0.01691	0.054	0	97.04	0.5271	276.3	0.126	1	10.29	10.87	1.479	14	16
0.0125	0.02703	4	3.538	67.87	0.01511	0.054	0	97.76	0.5848	301.3	0.126	1	10.87	10.87	1.519	14	16
0.0125	0.01923	5	3.195	58.22	0.01206	0.045	0	98.6	0.6614	346.7	0.108	1	11.47	10.87	1.612	14	16
0.0125	0.0125	6	2.829	48.41	0.009205	0.045	0	100.1	0.7973	417.9	0.09	1	13.51	10.87	1.756	14	16

Table 2 - Trade-off tuning table

3.4.3 - Base functions - Coincidence horizon

The position trajectories are defined as parabolas by the path or geometrical trajectory scheduler. The process being non integrative, 3 base functions : step, ramp and parabola are needed.

The final selection of the coincidence horizon (18 ms - 54 ms) is determined with the help of PFC matlab package with a reference trajectory defined by a time constant of 60 ms.

The oscillating mode is decomposed into 2 real modes. table (2) gives the trade-off between different criteria.

Selected values for a convenient trade-off were $\tau_1 = 19$ ms, $\tau_2 = 27$ ms.

3.4.4 - Anticipation

Position trajectory is known in advance (next to 200 ms). Anticipation is an interesting feature of PFC and used systematically to smooth MV and CV's behaviour. It consists in shifting to the future set point definition while still in the previous zone.

Setpoint (SP) is defined by spline curves between and T_i, T_{i+1}, (fig. 3.5).

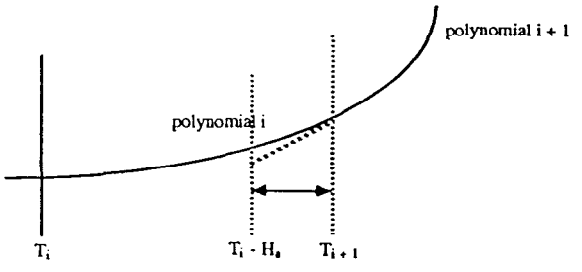

Figure 3.5 - Anticipation

Anticipation is to shift to parameters C^j_{i+1} between $T_{i+1} - H_a$, and T_{i+1}.

$$t \in [T_{i+1} - H_a, T_{i+2} - H_a[\quad (8)$$

$$SP(t) = C^0_{i+1} + C^1_{i+1}(t - T_{i+1}) + C^2_{i+1}(t - T_{i+1})^2 \quad (9)$$

Here H_a was selected at 19 ms. PFC goes to a look-up table and retains the computed spline parameters value C^j_i at time t + 19 ms.

3.4.5 - Constraints

The variator stalls if the speed setpoint is too high. The Mv_pfc is then limited by :

$$\pm|\dot{\theta}_{max}| = Mv\_pfc_{max}(n) - gbpos \cdot position(n) \quad (10)$$

$$Mv\_pfc_{max}(n) = \pm|\dot{\theta}_{max}| + gbpos \cdot position(n) \quad (11)$$

Viscous friction being small, the current constraint is roughly transformed into a speed constraint on the speed setpoint.

$$|Mv\_pfc(n) - Mv\_pfc(n-1)| < Mv\_pfc_{max}(n) \quad (12)$$

Elementary logic selects the worst condition and clips the Mv_pfc, while the internal value of the model is re-initialized on the contrained value.

3.4.6 - Results - Conclusion

Specifications are tough :

- robustness : for 0 kg or 20 kg, the same behaviour is looked for.
- dynamics : path dynamic accuracy should be better than ± 1 mn. Docking is finished when CV remains in a ± 0,2 mm channel around set point.
- target : minimize the time response. Fig. 3.6 and 3.7 show some recorded behaviours.

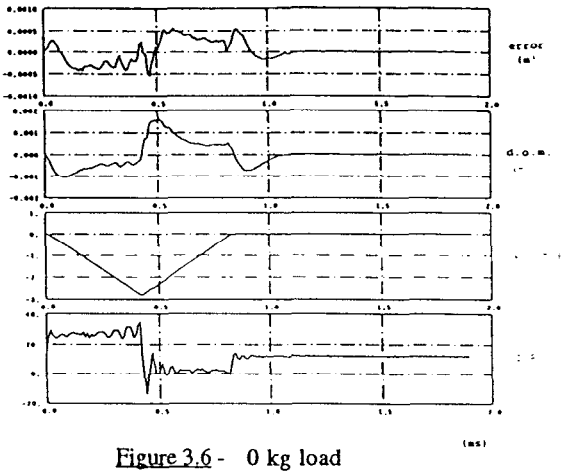

Figure 3.6 - 0 kg load
speed max 4 m/s
accel max 7 m/s^2

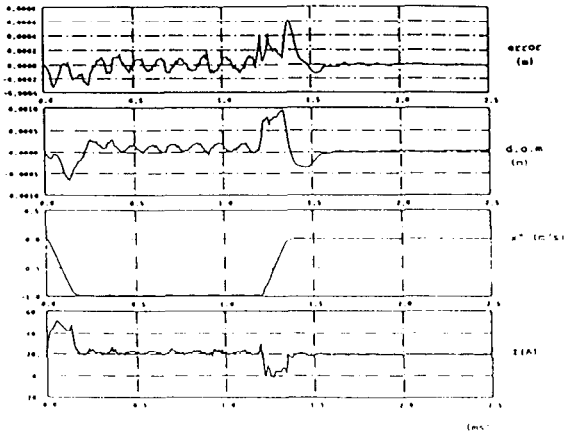

Figure 3.7 - Load 24 kg
speed max 7 m/s
accel max 12 m/s^2

- The main interest lies in the procedure :

  - Identification : a PC is connected to the robot, acquires signals, applies an optimal sensitizing protocol in a closed loop way. Global identification is performed on site, a simulator is tuned.

  - PFC design : CAD defines rapidly the decomposed modes (Reference trajectory is fixed at 60 ms). Anticipation is fixed around 20 ms. Constraints are very efficient and significant parameters to be tuned as secondary trade-off between performance and wear of the mechanical parts.

A local PC 486 controls the robot and a full evaluation is made in 45 minutes of time. Several loads and degrees of freedom are tested in the same day.

The future target is now to skip that tuning phase and to design the controller right away from a mechanical CAD design, on the original physical model, with a powerful work-station.

4 - RIVER LEVEL CONTROL

Between Geneva and the Mediterranean sea, 18 dams control the water levels and flows of the Rhône river. The "Compagnie Nationale du Rhône" (CNR) is in charge of the control of water levels, locks and electricity production.

Traditional PID control is to be improved to optimize performance (maximize electricity production), to take into account constraints and to facilitate the tuning of revamped or new facilities within the frame of normalized procedures.

A section of river is defined by a dam and a hydraulic power plant upstream, and a dam and a power plant downstream, plus a certain number of possible tributaries (figure 4.1).

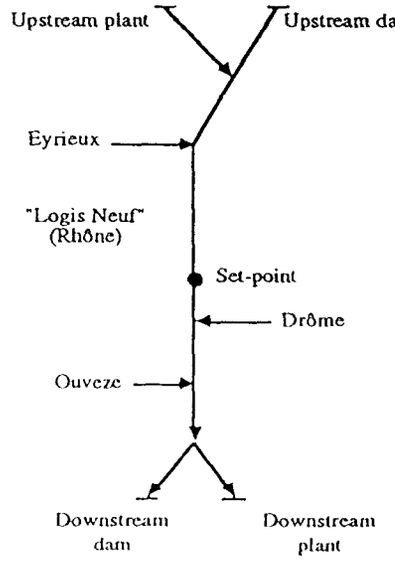

Figure 4.1 - River section (Logis Neuf)

The controlled variable is the level of water, in a well specified location, the manipulated variables are the down-stream dam and plant flows, the measured disturbances (figure 4.2).are the dam and plant up-stream flows and the tributaries flows. Unmeasured disturbances come from losses of water through river bed and banks, evaporation, unmeasured affluents and rain (figure 4.2).

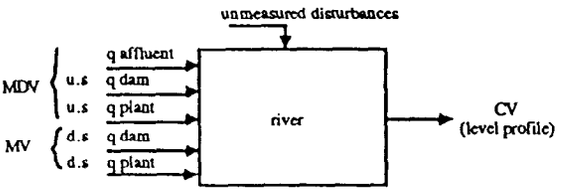

Figure 4.2 - Control configuration

The process appears to be the product of a classical integrator (flow - level) system, with time delay due to measurement location, by a non-well-behaved oscillatory process (waves) which depends on flow and level values.

If a plain performance is looked for, PID control is sufficient, provided it is tuned in a robust but sluggish way. Predictive control seemed a priori a well adapted procedure because :

- feed-forwarding is easy, here most of the perturbations are measured ;

- severe constraints affect both manipulated and controlled variables, and they are hit if the dynamic behaviour is to be improved.

CNR posseses a proprietary dynamic non-linear partial differential "first principles" model of the river, which is used anyway for the design of the different works. That model is tuned on site for every section. The river bed profile is measured and friction coefficients are estimated (Strikler parameters - [5]).

It seemed natural to use it as an internal model since sampling period of 5 minutes and 486 PC computer allows the use of such a model as an internal model today. No model reduction was thus necessary.

There is no particular difficulty, with the "independent model" approach, to use such a type of model. However the superposition theorem (free and forced mode) does not apply anymore, and classical incremental procedures cannot be used. Prediction should be made with a model whose state is realigned on the estimated state of the process.

In the linear case, even with state or structural perturbation, with or without error compensating procedure, there is in general no static error. In the non-linear case, these simplifying conditions are not valid anymore and a state estimating procedure is necessary. For industrial simplicity's sake it appeares convenient to use a classical approach which uses a "backward controller" as an estimator, and a "forward

controller" as an ordinary predictive controller. With the use of observability or reconstructability properties, if the outputs of process and model are alike during a certain horizon, depending on the order of the process, here selected as 5 samples, then internal states are alike, and the model input is the unknown disturbance. One elegant way to fulfil that matching requirement is to use a PFC with the process output as a set-point, the measured MV as a known disturbance, and to compute an MV (estimated equivalent lumped state and structural disturbance) such that $S_M(n) = CV(n)$ (figure 4.3).

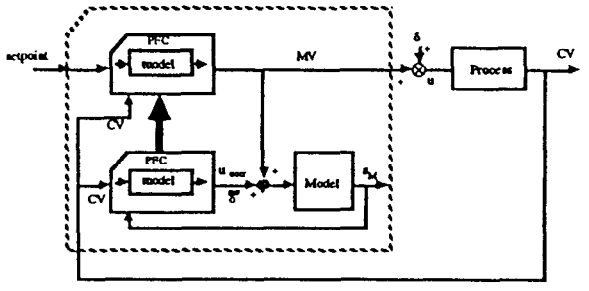

Figure 4.3 - Backward and forward controllers

It is to be noted that the internal model of the controller is identical to the process, such that robustness is not needed and that a perfect match on dynamic set-point, with no lag error, can be easily achieved if base functions are properly selected.

Base functions (here step and ramp), and coincidence horizon, are determined by PFC CAD procedure and tuned according to the nature of set point and the disturbances (parabolic function) (figure 4.4).

The reference trajectory has some importance by its implicit filtering effect on the process measurement noise.

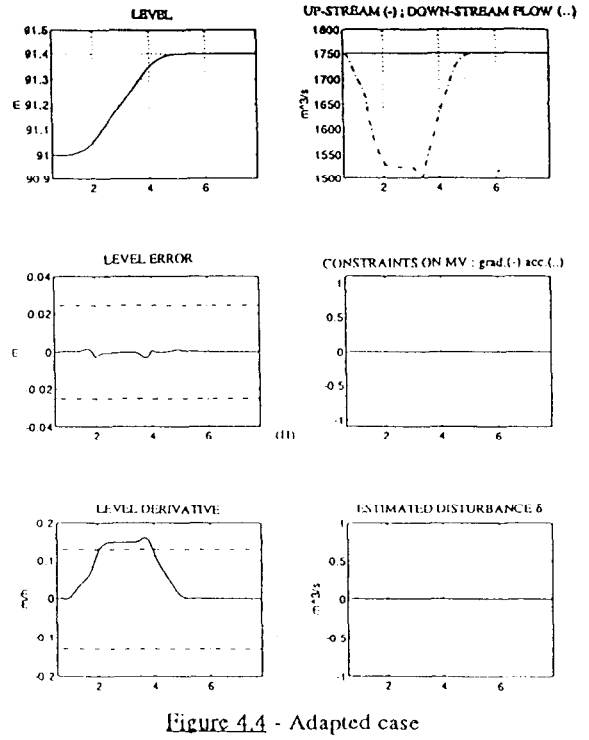

Figure 4.4 - Adapted case

The estimated state of process $\tilde{X}_p(n)$ is then transferred to the forward, usual, controller which will use a non-linear solver to compute the future response. The plant is submitted to an unknown but estimated disturbance $\tilde{\delta}(n)$, supposed to be at a constant during the coincidence horizon.

For simplicity's sake, if one considers only one base function (step) and one coincidence point H, if $y_R(n + H)$ is the reference trajectory target, and $y_M(n + H)$ the internal model output at time n + H, the problem is to find :

$$u(n) = u(n + i) \qquad (0 \le i < H)$$

such that :

$$y_M(\tilde{X}_p(n), u(n)) = y_R(n + H) \qquad (13)$$

A secant procedure can be used with a few iterations starting by :

$$u_1(n) = u(n - 1) \rightarrow y_M^1(n + H)$$
$$u_2(n) = u(n - 1) + \Delta u \rightarrow y_R^1(n + H)$$

giving :

$$u^*(n) = u_1(n) + \frac{y_R(n + H) - y_M^1(n + H)}{y_M^2(n + H) - y_m^1(n + H)} \cdot (u_2(n) - u_1(n)) \qquad (14)$$

2 or 3 iterations appear to be sufficient.

Constraints are taken into account on MV, they also reflect constraint on CV.

$$MV_{min} \le MV(n) \le MV_{max}$$

where $MV_{max, min}$, may depend on the state of the process.

$$\Delta MV(n) = MV(n) - MV(n - 1)$$
$$| \Delta MV(n) | < \Delta_L$$

Constraints limit the speed of variation of the level. If that constraint is not satisfied the banks of the river are rapidly washed away and destroyed. The valves of plant and dam should have smooth variations, with no alternating motion, not to create waves and hammering effects. Smoothness of MV's and CV's is a major criterion in acceptance tests.

Tests - Conclusion

In the adapted case, without any disturbance, a step change of level with limitation on speed and acceleration from 91 m to 91.4 m according a parabolic and ramp prescribed trajectory is described (fig. 4.4) (time scale : hours). One can notice smooth MVs and CVs. Constraints on MV gradient are noted ± 1 when hit, and ± 0.5 for acceleration.

In case of an unmeasured disturbance with a saw tooth profile (fig. 4.5) the backward controller estimates the perturbation and a maximum error of 7 cm can be observed, while constraints on gradient and acceleration of MV are hit during transient.

In the case of both model mismatch (dynamic is divided by 2) and state disturbance (fig. 4.6), the error is larger (25 cm), while manipulated flow remains smooth. Note that both MV's (plant and dam flows) act when constraints are hit.

Results were deemed quite satisfactory and implementation of the PFC controller in the general control procedure will be finished in 1994.

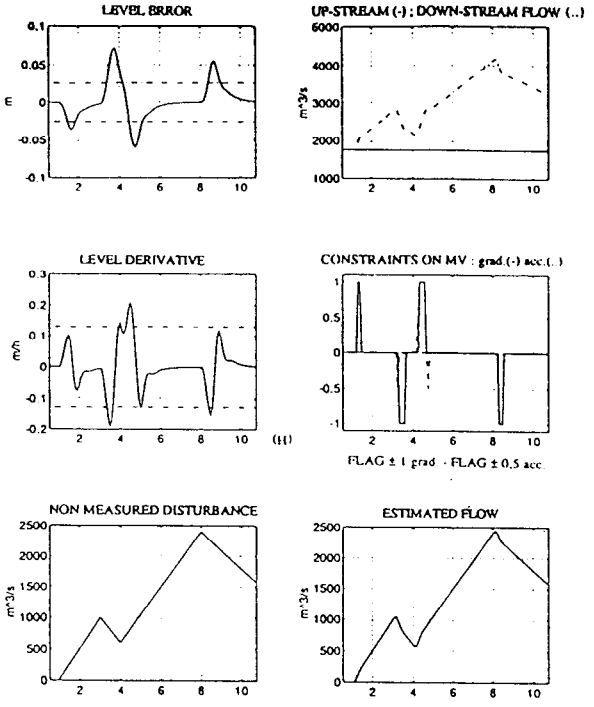

Figure 4.5 - State disturbance

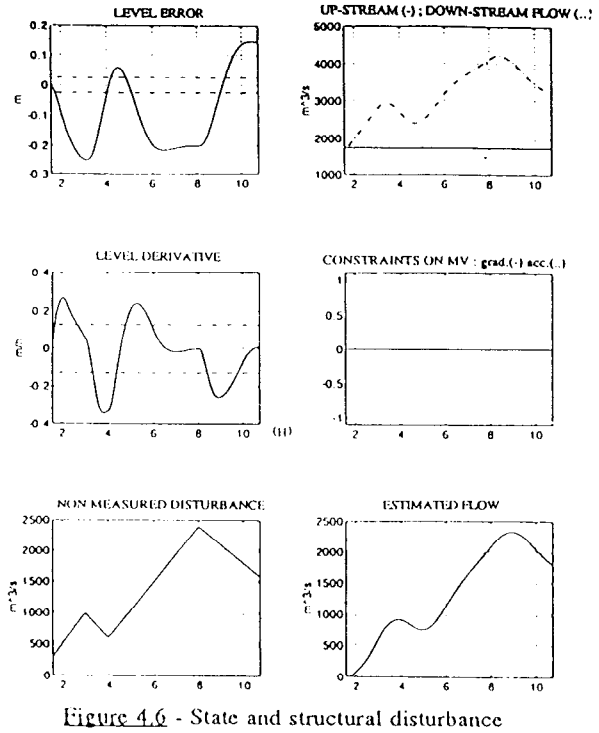

Figure 4.6 - State and structural disturbance

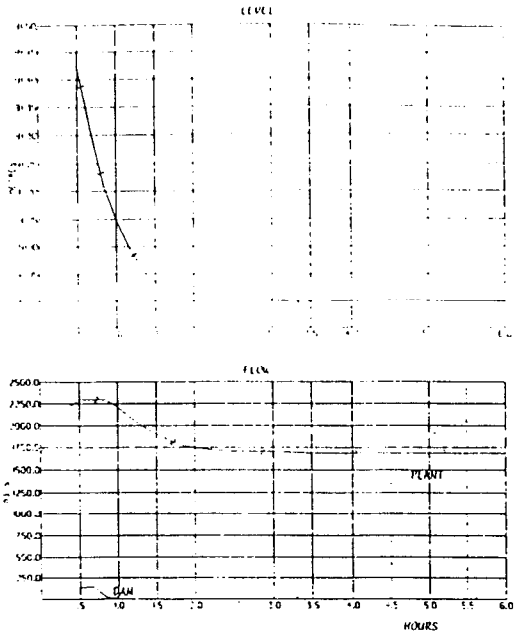

Figure 4.7 - Set point change - PFC

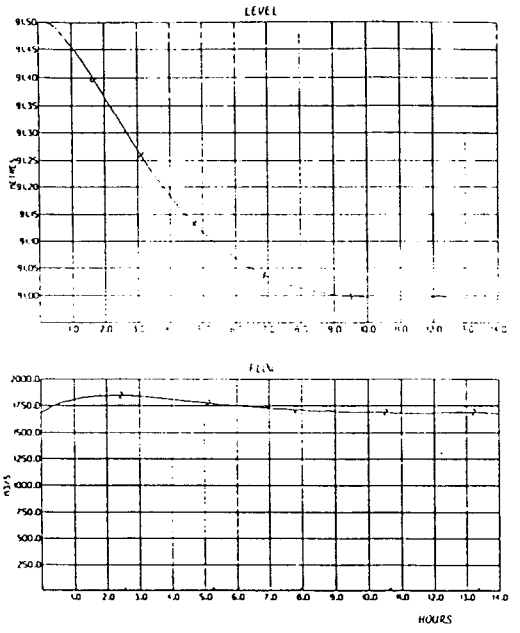

Figure 4.8 - Set point change - PID

5 - GENERAL CONCLUSION

There will always be a need for improvements in identification and predictive control : complex constraints, unstable systems, large mechanical systems with many flexible modes, etc ... However we now have efficient packages and a "reliable methodology" so that progress may also come from other aspects of the general procedure.

The true target is to **eliminate the control engineer** by offering chemical and mechanical engineers the appropriate control know-how, supported by well-packaged CAD technologies (different from tool-boxes), so that they might be able to handle the design trade-offs by themselves.

Integrated Design can be a part of Concurrent Engineering, physical design parameters will interact and merge with control parameters. Control will then contribute at a different and higher level.

BIBLIOGRAPHY

[1] S. Abu el Ata-Doss, P. Fiani and J. Richalet (1991). *Handling input and state constraints in predictive functional control*, CDC, Brighton.

[2] R.R. Bitmead, M. Gevers and V. Wertz (1990). *Adaptive optimal control : the thinking man's GPC*, Prentice Hall.

[3] E.F. Camacho (1991). *Constrained generalized predictive control*, IEEE Trans. AC, vol 38, n° 2.

[4] D.W. Clarke (1993). *Advances in Model-Based Predictive Control*, in Advances in Model-Based Predictive Control. Conference Oxford, Vol 1, pp 3-23.

[5] J.A. Cunge, F.M. Holly and A. Virwey (1980). *Practical aspects of computational river hydraulics*, Pitman.

[6] A. De Luca, A. Isidori and F. Nicolo (1985). *Control of robot arm with elastic joints via nonlinear dynamic feedback*, Proc. 24th Conf. Dec. Control., Fort Lauderdale, U.S.A., pp1671-1679.

[7] D. Fapiano and D. Steeper (1983). *Thickness control in cold rolling*, Iron and Steel Engineer, Nov.

[8] M.P. Hennessey, J.A. Priebe, P.C. Huang and R.J. Grommes (1987). *Design of a light weight robotic arm and controller*, Proc. IEEE Conference on Robotics on Automation, Raleigh, pp 779-785.

[9] I. Hoshino, Y. Maekawa, T. Fujimoto, Hir. Kimura and Hid. Kimura (1988). *Observer-based multivariable control of the aluminium cold tandem mill*, Automatica, vol 24, n° 6, pp 741-754.

[10] A.G. Longmuir (1974). *Dynamic control of multi-stand aluminium cold rolling mills*. Proc. 4th IFAC/IFIP International Conf. on Digital Computer Applications to Process Control, Part II, Zürich, pp 25-38.

[11] D.Q. Mayne and H. Michalska (1990). *Receding horizon control of nonlinear systems*, IEEE Trans. AC, vol 35, n° 7, pp 814-824.

[12] J. Richalet (1991). *Pratique de l'Identification*, Hermès.

[13] J. Richalet (1993). *Pratique de la Commande Predictive*, Hermès.

[14] J. Richalet (1993). *Industrial applications of Model Based Predictive Control*, Automatica, vol 29, n° 5, pp 1251-1274.

[15] R. Scattolini and S. Bittani (1990). *On the choice of the horizon in long-range predictive control - some simple criteria*, Automatica, vol 26, n° 5, pp 915-917.

[16] S. Yurkovich, F.E. Pachero and A.P. Tzes (1989). *On-line frequency domain information for control of a flexible-link robot with payload*, IEEE Transactions on Automatic Control, vol 33, pp 1300-1303.

[17] S. Yurkovich, A.P. Tzes and K.L. Hillsley (1990). *Modeling and control issue for a manipulator with two flexible links*, Proc. 29th IEEE Conf. on Decision and Control, Honolulu, pp1995-2000.

[18] E. Zafiriou (1991). *On the robustness of model predictive controllers*, 4th Int. Conf. on Chemical Process Control, South Padre Island, Texas.

ANNEX B

- pfcsnl.m : control algorithm in matlab langage (level 1)
- calopt.m : control algorithm in matlab langage (level 2)
- comnl.c : control algorithm in C langage (level 1 and 2)
- comnl.h : parameters of the control algorithm
- funcalc.c : calculation functions used in the control algorithm
- proto.h : declaration of the functions

```
function [sor,x0]=pfcsnl(tn,x,ent,flag,param)

global flinit

if flag==0,
   sor=[0 1 1 4 0 1];
   x0=param(2);

%> Etats Discrets  x(n+1)   ----------------------------------------------------
elseif abs(flag)==2,
  if abs( round(tn/param(1))-(tn/param(1)) ) < sqrt(eps),
     %> Entree
     Cons_prod=ent(1);
     qe=ent(2);
     xbio=ent(3);
     Fr=ent(4);
     Prod=qe*xbio;
     xm=xbio;
     flinit==1;

   %> Calcul de la commande
     if flinit==1
        flinit=0;
        sor =param(2);
     else
        Hc=2.5; lam=.75;
        nHc=round(Hc/param(1));

        % reference
        yr=Cons_prod-lam^nHc*(Cons_prod - Prod);

        % scenario
        FRmin=10;FRmax=400;
           delFr=5*sign(Cons_prod-Prod);
           T=(0:param(1):Hc)';
           QEcom=qe*ones(size(T));
           FR0com=Fr*ones(size(T));
           FR1com=(Fr+delFr)*ones(size(T));
           [t,x,y]=rk45('mods',Hc,xm,[1e-5 1e-2 1e1 0 3 2],[T FR0com QEcom],xm);
           y0=y(length(y));
           [t,x,y]=rk45('mods',Hc,xm,[1e-5 1e-2 1e1 0 3 2],[T FR1com QEcom],xm);
           y1=y(length(y));

           sor=Fr+(yr-y0)/(y1-y0)*delFr;
           sor=min(FRmax,max(sor,FRmin));
     end

  else
     sor = x;
  end

%> Sorties du systeme   ---------------------------------------------------------
elseif flag==3,
  sor = x;

%> Instant du prochain appel   --------------------------------------------------
elseif flag==4,
  ns = tn/param(1);            % nombre de simulation
  sor = param(1) * (1  + floor(ns + 1e-13*(1+ns)));

%> ------------------------------------------------------------------------------
else
  sor = [];
end
```

```
function [y]=calopt(u)

% entrees de la fonction
% ----------------------
Cons_prod=u(1);          % consigne de production demandee
qe=u(2);                 % debit nominal demande

% contraintes a rsepecter
% -----------------------
Xmax=1.5; Xmin=0.5;      % contraintes sur la concentration
qmax=qe*1.1;             % debit max autorise
qmin=qe*0.9;             % debit min autorise

% calcul de la consigne de production respectant les contraintes
% --------------------------------------------------------------
cons=max(min(Cons_prod,Xmax*qmax),Xmin*qmin);

% calcul du debit optimum
% -----------------------
q=qe;
if (cons/Xmax > qe), q=min(qmax,cons/Xmax);end
if (cons/Xmin < qe), q=max(qmin,cons/Xmin);end

% sorties de la fonction
% ----------------------
y(1)=cons;                % consigne de production realisable
y(2)=q;                   % debit optimum
```

```
#include "comnl.h"
#include "math.h"
#include "proto.h"

/*
   COMNL.C   Algorithme du regulateur non lineaire.
   ESA - MELISSA - SPIRULINE

   Date: 15-DEC-94
*/

/* Declaration des variables statiques */
   static double frmem;


/* ---  COMNL0   ------------------------------------------------------
   Fonction:
      Initialisation du regulateur non lineaire
   Synopsis:
      COMNL0(FR)
   Description:
      Affecte la valeur initiale FR
*/
double comnl0()

{
double   fr ;
fr = frinit;
frmem = fr;
return(fr);
}

/* ---  COMNL    ------------------------------------------------------
   Fonction:
      Equations du regulateur non lineaire
   Synopsis:
      COMNL(CONS_PROD,CXA,QE,FR)
   Description:
      Calcul la commande courante FR a partir de
      la mesure de concentration CXA, de la consigne CONS_PROD, du
      debit QE
*/
double comnl(cons_prod,cxa,qe)

double   cons_prod, cxa, qe ;
{
/* declaration des variables internes */
   double   prod, dil, prod_ref, delfr;
   double   fr , fr1, fr2, prod1, prod2;
   double   qe_max , qe_min , prod_max , prod_min ;

   prod = cxa*qe;

qe_max = qe*(1+dq);
qe_min = qe*(1-dq);
prod_max = qe_max*cxa_max;
prod_min = qe_min*cxa_min;
cons_prod = max(prod_min,min(prod_max,cons_prod));
if (cons_prod/cxa_max > qe )
   {
   qe = min(qe_max,cons_prod/cxa_max);
   }
if (cons_prod/cxa_min < qe )
   {
```

```
    qe = max(qe_min,cons_prod/cxa_min);
    }

    dil = qe/vol;

/* trajectoire de reference */
    prod_ref = cons_prod - pow(lambda,nhc)*(cons_prod - prod);

/* commande precedente */
    fr = frmem;

/* premier scenario */
    fr1 = fr;
    prod1 = model(cxa,fr1,dil);

/* deuxieme scenario */
    delfr = dfr*sign(cons_prod - prod);
    fr2 = fr1 + delfr;
    prod2 = model(cxa,fr2,dil);

/* calcul de fr */
    fr+ = (prod_ref - prod1)/(prod2 - prod1)*delfr;

/* contraintes sur fr */
    fr = max(fr_min,min(fr_max,fr));

/* memorisation */
    frmem=fr;
    return(fr);
}
/* ---  MODEL  ------------------------------------------------------------
    Fonction:
          integration du modele
    Synopsis:
          MODEL(CXA,FR,DIL,PROD)

*/
double model(cxa,fr,dil)

double cxa, fr, dil ;

{
    double v, dv, vout , prod;
    int k;

    v = cxa;
    for (k=1 ; k <= nhc; k++)
        {
        dv = dercx(v,fr,dil);
        vout =v + dt *dv;
        v=vout;
        }
    prod=vout*dil*vol;
    return (prod);
}


/* --- DERCX ------------------------------------------------------------

    Fonction:
          calcul de la derivee de cxa
    Synopsis:
          DERCX(cxa,fr,dil,dvt);
```

```
*/
double dercx(cxa,fr,dil)

double cxa, fr, dil;

{
double  dcxdt;
double za, alpha, delta, pij, pijz;
double z, rxa;
za = zpc + zch;

alpha = sqrt(za*Ea/(za*Ea+(1+zg)*Es));
delta = (za*Ea+(1+zg)*Es)*alpha*RT*cxa;

pij = 0.;
for (z=jstep/2; z<=1-jstep/2; z+=jstep)
    {
    pijz = fr/z*2*cosh(delta*z)/(cosh(delta)+alpha*sinh(delta));
    if (pijz>=1)
       {
       pij+ = 2*z*pijz/(Kj+pijz)*jstep;
       }
    }
rxa = muM*pij*zpc*cxa*wiv;

dcxdt = -dil*cxa + rxa ;
return (dcxdt);
}
```

```
#include "math.h"

/* ---   MIN.C   ------------------------------------------------------------
   Fonction:
         Minimum de deux valeurs.
   Synopsis:
         X=MIN(Y,Z)
*/
double min( x1 , x2 )

double x1 , x2;
{
   double  x;
   x = (x1 < x2) ? x1 : x2;
   return( x );
}

/* ---   MAX.C   ------------------------------------------------------------
   Fonction:
         Maximum de deux valeurs.
   Synopsis:
         X=MAX(Y,Z)
*/
double max( x1 , x2 )

double x1 , x2;
{
   double  x;
   x = (x1 > x2) ? x1 : x2;
   return( x );
}

/* ---   SIGN.C   -----------------------------------------------------------
   Fonction:
         signe d'une valeur.
   Synopsis:
         X=SIGN(Y)
*/
double sign( y )

double y;
{
   double  x;
   x = (y < 0) ? -1. : 1.;
   return( x );
}
```

```
/*
   Nom : comnl.h

   Fonction : Coefficients de la commande

   Date : 15-DEC-94
*/

#define dt          0.5       /* control period (in h ) */
#define nhc         5.        /* coincidence point (in dt) */
#define lambda      0.75      /* reference trajectory dynamic */
#define dfr         5.        /* radiant flux increment (in W/m2)  */
#define fr_min      10.       /* min constraint on FR (in W/m2) */
#define fr_max      400.      /* max constraint on FR (in W/m2) */
#define dq          10.       /* flow variation (in %) */
#define cxa_min     0.5       /* min constraint on CXA (in g/l) */
#define cxa_max     1.5       /* max constraint on CXA (in g/l) */
#define vol         7.        /* reactor volume */

#define zpc         .162      /*    */
#define zch         .01       /*    */
#define zg          0.1       /*    */
#define Ea          871.      /*    */
#define Es          167.      /*    */
#define RT          .048      /*    */
#define Kj          20.       /*    */
#define muM         .54       /*    */
#define wiv         .52       /*    */
#define jstep       .01       /*    */

#define frinit      200.      /*    */
```

```
double comnl( );
double comnl0( );
double model( );
double dercx( );
double sign( );
double min( );
double max( );
```